FACULDADE DE CIÊNCIAS
UNIVERSIDADE DO PORTO

ICBAS | INSTITUTO DE CIÊNCIAS BIOMÉDICAS ABEL SALAZAR
SCHOOL OF MEDICINE AND BIOMEDICAL SCIENCES

MSc

2.º CICLO

FCUP
ICBAS
2022

Molecular mechanisms involved in Transthyretin Amyloidosis

Ana Margarida Caetano Gomes

MSc

FACULDADE DE CIÊNCIAS
UNIVERSIDADE DO PORTO

ICBAS | INSTITUTO DE CIÊNCIAS BIOMÉDICAS ABEL SALAZAR
SCHOOL OF MEDICINE AND BIOMEDICAL SCIENCES

Molecular mechanisms involved in Transthyretin Amyloidosis

Ana Margarida Caetano Gomes

Dissertação de Mestrado apresentada à
Faculdade de Ciências da Universidade do Porto e ao Instituto de Ciências Biomédicas Abel Salazar da Universidade do Porto em Bioquímica

2022

MSc

Molecular mechanisms involved in Transthyretin Amyloidosis

Ana Margarida Caetano Gomes
Mestrado em Bioquímica
Faculdade de Ciências da Universidade do Porto
Instituto de Ciências Biomédicas Abel Salazar, Universidade do Porto
2022

Orientadora
Professora Doutora Maria do Rosário Almeida,
Professora Associada,
Instituto de Ciências Biomédicas Abel Salazar, Universidade do Porto

U.PORTO

FACULDADE DE CIÊNCIAS
UNIVERSIDADE DO PORTO

U.PORTO

ICBAS | INSTITUTO DE CIÊNCIAS BIOMÉDICAS ABEL SALAZAR
SCHOOL OF MEDICINE AND BIOMEDICAL SCIENCES

Todas as correções determinadas pelo júri, e só essas, foram efetuadas.

O Presidente do Júri,

Porto, _____/_____/_____

À minha família

Declaração de Honra

Eu, Ana Margarida Caetano Gomes, inscrita no Mestrado em Bioquímica da Faculdade de Ciências da Universidade do Porto declaro, nos termos do disposto na alínea a) do artigo 14.º do Código Ético de Conduta Académica da U.Porto, que o conteúdo da presente dissertação reflete as perspetivas, o trabalho de investigação e as minhas interpretações no momento da sua entrega.

Ao entregar esta dissertação, declaro, ainda, que a mesma é resultado do meu próprio trabalho de investigação e contém contributos que não foram utilizados previamente noutros trabalhos apresentados a esta ou outra instituição.

Mais declaro que todas as referências a outros autores respeitam escrupulosamente as regras da atribuição, encontrando-se devidamente citadas no corpo do texto e identificadas na secção de referências bibliográficas. Não são divulgados na presente dissertação quaisquer conteúdos cuja reprodução esteja vedada por direitos de autor.

Tenho consciência de que a prática de plágio e auto-plágio constitui um ilícito académico.

Ana Margarida Caetano Gomes

Porto, 30 setembro 2022

Agradecimentos

Neste espaço, gostaria de expressar a minha profunda gratidão a todos os que estiveram envolvidos neste meu percurso académico.

À Professora Doutora Maria do Rosário Almeida, orientadora deste trabalho, que me possibilitou fazer parte deste projeto. Agradeço todo o seu incentivo, a muita disponibilidade, dedicação, paciência e maravilhosas conversas que me permitiram evoluir pessoal e academicamente.

À Professora Doutora Maria João Saraiva, líder do grupo de Neurobiologia Molecular, por me ter acolhido no seu grupo.

À Professora Doutora Isabel Cardoso por toda a sua disponibilidade e ajuda.

Aos meus colegas de laboratório, Anabela, Beatriz, Filipa, Joana, João G., João M., Lúcia, Mariana, Tiago G., Tiago T. e Sofia, um especial agradecimento por toda a ajuda que me facultaram bem como pelos bons momentos que passamos juntos. Um agradecimento especial para a Joana, o Tiago G. e a Mariana.

Aos meus colegas de mestrado, principalmente à Saulė e à Sara, mas também à Eduarda, ao Guilherme e à Rosa pelas nossas conversas de corredor.

À minha amiga de sempre, Marlene, pelo apoio constante.

E um agradecimento muito especial à minha família que sempre me apoiou incondicionalmente em todas as minhas escolhas e que me dão forças para seguir em todas as minhas aventuras. Muito obrigada!

Resumo

Amiloidose é um grupo de doenças que em comum apresentam a agregação de proteínas extracelulares instáveis e a formação e deposição de fibrilas amiloides em todos os tecidos. A transtirretina (TTR) é uma dessas proteínas instáveis com propensão amilóide e está associada a dois tipos diferentes de doença: amiloidose por transtirretina hereditária (amiloidose ATTRv) e amiloidose por transtirretina *wild type* (amiloidose ATTRwt).

O mecanismo preciso da amiloidogénese da ATTR ainda não é completamente conhecido, mas a formação de amiloide requer a desestabilização da proteína e o seu desenrolamento parcial, e em algum momento, a proteólise da TTR também pode ocorrer.

Para contribuir para o conhecimento da relevância da proteólise na doença e os mecanismos moleculares associados, este trabalho teve como principais objetivos: caracterizar os níveis de Serpina3n em ratinhos HM30 e compará-los com ratinhos controlo; caracterizar a agregação da TTR wt em condições de proteólise e clarificar o seu efeito na linha celular de cardiomiócitos HL-1; e caracterizar a agregação da TTR wt, TTR L55P, TTR V122I e do fragmento TTR 49-127 não submetidos à proteólise e elucidar o seu efeito em cardiomiócitos HL-1.

Detetámos níveis de expressão semelhantes de Serpina3n quer no fígado quer no coração, embora os níveis de proteína no fígado tenham sido inferiores quando comparados com os ratinhos controlo. No plasma, os níveis de Serpina3n foram mais elevados nos ratinhos HM30 do que nos controlos, o que pode ser devido ao aumento da secreção de Serpina3n do fígado, associado ao seu papel de chaperona na amiloidose de TTR.

Considerando estudos de agregação de TTR na presença de proteólise, confirmamos a redução da atividade da plasmina com a TTR wt e o efeito da SerpinA1 é provavelmente devido à inibição da plasmina. Não observamos diferenças nos níveis dos diferentes marcadores de doença estudados quando incubadas as diferentes espécies agregadas em cardiomiócitos HL-1, sugerindo que 24 horas de agregação não foram suficientes para formar número suficiente de pequenos agregados de TTR wt que pudessem perturbar a homeostase celular.

Em relação aos estudos de agregação de TTR sem proteólise, confirmamos a propensão amiloidogénica das diferentes variantes de TTR, a ordem de menor para

maior propensão a agregar foi TTR wt, TTR V122I, TTR L55P e fragmento TTR 49-127. Todas as amostras de proteínas apresentaram alta complexidade no que diz respeito às diferentes espécies oligoméricas em solução. Os estudos celulares apresentaram algumas inconsistências, mas a autofagia e o stresse do RE foram alterados devido às formas de TTR agregadas.

Apesar de todas as limitações dos estudos *in vitro* e celulares, eles são importantes para o conhecimento detalhado do mecanismo de agregação da TTR, uma vez que o envolvimento de fatores específicos pode ser direcionado para modulação visando abordagens terapêuticas, e sistemas simples permitem identificar tais fatores e permitem testar moduladores.

Palavras-chave: Transtirretina, amiloidose, Serpins, chaperonas, proteólise, agregação de proteínas, enrolamento de proteína, cardiomiócitos, autofagia, stress do retículo endoplasmático

Abstract

Amyloidosis is a group of diseases that in common have the aggregation of extracellular unstable proteins and formation and deposition of amyloid fibrils in all tissues. Transthyretin (TTR) is one of those unstable proteins with amyloid propensity and is associated with two different types of disease: hereditary transthyretin amyloidosis (ATTRv amyloidosis) and wild type transthyretin amyloidosis (ATTRwt amyloidosis).

The precise mechanism of ATTR amyloidogenesis is still not completely known, but amyloid formation requires protein destabilization and partial unfolding, and at some point TTR proteolysis may also occur.

To contribute to the knowledge of relevance of proteolysis in amyloidosis pathogeny and the associated molecular mechanisms this work had as main objectives: to characterize HM30 mice regarding Serpina3n levels and compare them to control mice; to characterize TTR wt aggregation under proteolytic conditions and to elucidate the effect of these TTR wt aggregates in the HL-1 cardiomyocyte cell line; and to characterize TTR wt, TTR L55P, TTR V122I and TTR fragment 49-127 aggregation not submitted to proteolysis and to elucidate the molecular mechanisms involved in the cellular response to these TTR aggregates (not submitted to proteolysis) in the HL-1 cardiomyocytes.

We found similar expression levels of Serpina3n mRNA in both, liver and heart tissues, although, protein levels were found decreased in the liver, and in plasma, HM30 mice presented higher levels than controls, which could be due to increased Serpina3n secretion from liver associated with its role as a TTR chaperone in ATTR amyloidosis.

Considering TTR aggregation studies in the presence of proteolysis, we confirmed the reduced plasmin activity with TTR wt and the effect of SerpinA1 is probably due to inhibition of plasmin. We did not observe differences in the levels of the different disease markers studied when incubated the different aggregated species in HL-1 cardiomyocytes, suggesting that 24 hours of aggregation were not sufficient to form enough small TTR wt aggregates that could perturb the cell homeostasis.

Regarding TTR aggregation studies without proteolysis, we confirmed the amyloidogenic propensity of the different TTR variants, the order of increased propensity to aggregate was TTR wt, TTR V122I, TTR L55P and TTR 49-127 fragment (TTR wt was the least amyloidogenic form). And all protein samples presented high complexity in what concerns the different oligomeric species in solution. Cellular studies presented some inconsistencies, but autophagy and ER stress are altered due to aggregated TTR forms.

Despite all limitations of *in vitro* and cellular studies, they are important for the detailed knowledge of the TTR mechanism of aggregation, since the involvement of specific factors can be targeted for modulation aiming therapeutic approaches and simple systems permit to identify such factors and allow to test modulators.

Keywords: Transthyretin, amyloidosis, serpins, chaperones, plasmin, proteolysis, protein aggregation, protein folding, cardiomyocytes, autophagy, endoplasmic reticulum stress

Table of Contents

Tables List

Figures List

Abbreviation List

ALS	Amyotrophic Lateral Sclerosis
apoA-I	Apolipoprotein A-I
ATTR amyloidosis	Transthyretin Amyloidosis
ATTRv amyloidosis	Hereditary Transthyretin Amyloidosis
ATTRwt amyloidosis	wild type Transthyretin Amyloidosis
Aβ	Amyloid-β
BiP	Binding immunoglobulin Protein
BMP-10	Bone Morphogenic Protein 10
BSA	Bovine Serum Albumin
CNS	Central Nervous System
CSF	Cerebrospinal Fluid
cTnT	cardiac Troponin T
DEAE	Diethylaminoethyl
DLS	Dynamic Light Scattering
DMEM	Complete Dulbecco's Modified Eagle's Medium
ECL	Enhanced Chemiluminescent
ER	Endoplasmic reticulum
EGCG	Epigallocatechin-3-gallate
ERAD	ER-associated degradation
FAC	Familial Amyloid Cardiomyopathy
FAP	Familial Amyloid Polyneuropathy
FBS	Fetal Bovine Serum
GAPDH	Glyceraldehyde 3-phosphate dehydrogenase
HBSS	Hanks' Balanced Salt Solution
HRP	Horseradish Peroxidase
Hsf1	Heat shock transcription factor 1
IGF1	Insulin-like growth factor 1 receptor
IPTG	isopropyl β-D-thiogalactopyuranoside
LB	Luria-Bertani
LRP-1	Lipoprotein-related receptor 1
NMR	Nuclear Magnetic Resonance
NPY	Neuropeptide Y
PBS	Phosphate Buffered Saline
PBST	Phosphate Buffered Saline with Tween

PC	Primary Cardiomyocytes
PCR	Polymerase Chain Reaction
qRT-PCR	Quantitative Real-Time PCR
RBP	Retinol Binding Protein
RCL	Reactive Centre Loop
RIPA	Radioimmunoprecipitation assay
RQI	RNA Quality Indicator
RT	Room Temperature
SDS-PAGE	Sodium Dodecyl Sulfate Polyacrylamide Gel Electrophoresis
SEM	Standard Error of the Mean
Serpina3n	Serine protease inhibitor A3n
SSA	Senile Systemic Amyloidosis
T4	Thyroxine
TDP-43	Transactive response DNA binding Protein 43 kDa
TEM	Transmission Electron Microscopy
ThT	Thioflavin T
TTR	Transthyretin
TTR wt	wild type Transthyretin
UPR	Unfolded Protein Response
WB	Western Blot
δ-GABA$_A$	δ-γ-aminobutyric acid A receptor

Introduction

The main objective of this master's project was to contribute to a better knowledge of the molecular mechanisms involved in Transthyretin Amyloidosis (ATTR amyloidosis).

Corino de Andrade, in 1952, described for the first time the Portuguese form of the disease that he designated paramyloidosis, and since then, many efforts have been made to comprehend the mechanism of transthyretin (TTR) amyloidogenesis, however, its precise mechanism is still not completely known[1,2]. However it is clear that TTR amyloid formation requires protein destabilization and partial unfolding, and at some point TTR proteolysis may also occur[1].

1. Amyloidosis

Life without proteins is impossible, so comes as no surprise that their synthesis is a very controlled process. Live organisms have a complex machinery to ensure that proteins have the right sequence, folding, destination… but folding is a matter of physical interactions, and sometimes the conformation of minimal energy is not the one that is the most functional. For some still unknown reason, some proteins, after the correct folding, misfold and form aggregates which may lead to the formation of insoluble fibrils.

These protein aggregates are in the genesis of several neurodegenerative diseases as Alzheimer's (Amyloid-β (Aβ) peptide and Tau protein), Parkinson's (α-synuclein), Huntington's (huntingtin), Amyotrophic Lateral Sclerosis (ALS, TDP-43 protein)[3]… in these examples, with exception of Alzheimer due to Aβ peptide, the diseases are due to aggregation of intracellular proteins. When aggregation occurs with extracellular proteins we observe local or systemic deposits giving rise to amyloidosis[4].

Amyloidosis is a group of diseases that in common have the aggregation of extracellular unstable proteins (with high propensity to aggregate) which lead to the formation of insoluble fibrils (amyloid) that deposit in several organs and tissues[1,3,5]. These proteins differ substantially in their primary structure but possess an extensive β-sheet conformation[1]. More than 30 proteins are known to form amyloid, in humans, and one of which is TTR[4].

1.1 Transthyretin Amyloidosis (ATTR amyloidosis)

TTR is associated with two different types of ATTR amyloidosis: Hereditary Transthyretin Amyloidosis (ATTRv amyloidosis), and wild type Transthyretin Amyloidosis (ATTRwt amyloidosis)[5]. According to the predominant clinical manifestations ATTRv amyloidosis can be classified as Familial Amyloid Polyneuropathy (FAP) or as Familial Amyloid Cardiomyopathy (FAC). In the case of the sporadic form of the disease related to ATTRwt, previously known as Senile Systemic Amyloidosis (SSA), the predominant clinical phenotype is cardiomyopathy[5].

ATTRv amyloidosis is related to single amino acid substitutions due to point mutations in the *TTR* gene, more than 150 different mutations in the coding region of this gene were described in ATTRv patients[6]. The North of Portugal is an endemic region, the Portuguese population harbors a focus of hereditary ATTR V30M amyloidosis[5,6]. Hereditary ATTR V30M amyloidosis is the most frequent ATTRv amyloidosis in Portugal, Spain, France, Switzerland, Germany, Sweden, Brazil and Japan[7]. Hereditary ATTR I68L amyloidosis is the most frequent in Italy[7]. In Denmark the most frequent is ATTR L111M amyloidosis[7]. In the United Kingdom and Ireland is ATTR T60A amyloidosis but in London as well as in Western Africa, United States of America and in the Caribbean is ATTR V122I amyloidosis[7].

ATTRwt amyloidosis is an age related disease and its incidence and prevalence are still unknown, however it is believed to be underestimated by clinicians resulting in misdiagnoses[7,8]. In an Asian study, in Japanese population (above 80 years old) its prevalence reached 12% (in a total of 26 individuals), and in a European study, in Finnish population (above 85 years old) its prevalence reached the 25% (in a total of 256 individuals)[9,10].

1.2 Clinical Manifestations

ATTR amyloidosis has a wide spectrum of clinical symptoms. This heterogeneous clinical expression, probably also conditioned by individual conditions of patients, turns its clinical characterization difficult and prone to misdiagnosis.

The most prevalent clinical features are cardiomyopathy and polyneuropathy. Despite some mutations being considered predominantly polyneuropathic (as TTR V30M, early age of onset) or cardiomyopathic (as TTR V122I), due to patients' main clinical manifestations, commonly ATTRv amyloidosis presents a mix of polyneuropathy and

cardiomyopathy (Figure 1). However, ATTRwt amyloidosis is considered mainly cardiomyopathic.

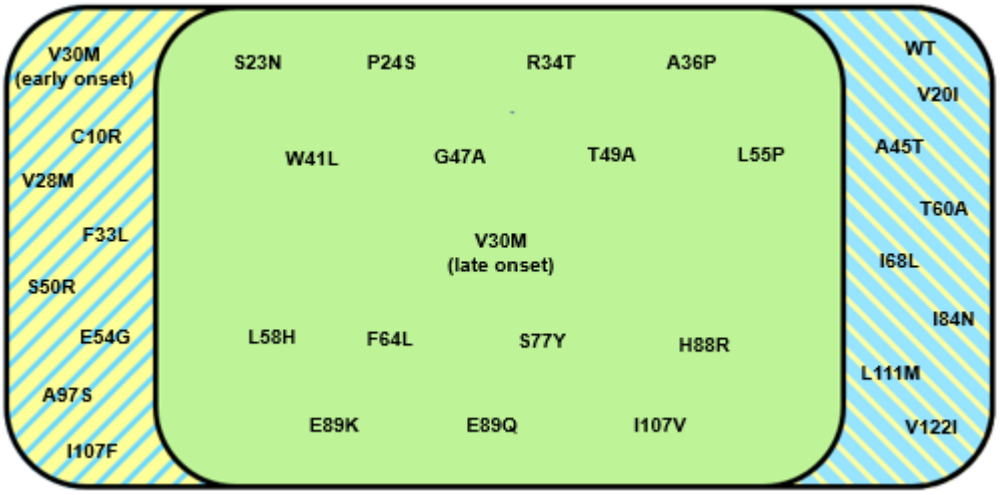

Figure 1 – Genotype-phenotype (polyneuropathy and/or cardiomyopathy) correlation in ATTR amyloidosis. WT: wild type TTR. ATTR amyloidosis mainly polyneuropathic. ATTR amyloidosis mainly cardiomyopathic. Mixed phenotype[5,11,12,13].

ATTRv amyloidosis due to TTR V30M mutation has two designations, early and late age of onset. ATTR V30M early onset amyloidosis is when patients develop the disease between the ages of 20 and 40 years old, while ATTR V30M late onset amyloidosis is when patients develop the disease at 50 years or older, what is behind the age of onset difference is still unknow. ATTR V30M patients from Portugal, Brazil and Kumamoto and Nagano (endemic areas in Japan) mainly present an early onset of the disease, while ATTR V30M patients from Sweden and from nonendemic areas in Japan present late onset of the disease[6].

Despite the most prevalent ATTR amyloidosis clinical features are polyneuropathy or/and cardiomyopathy, these are not the only phenotypes present in patients. As previously mentioned, ATTR is a systemic disease, protein aggregates/fibrils may deposit in several tissues and organs including the autonomic nervous system, the carpus, the gastrointestinal tract, the eye, the spine, and less frequent TTR variants may affect the central nervous system (CNS), leading to different and variable clinical manifestations which sometimes culminates in a difficult diagnosis (Figure 2). CNS symptoms are related to leptomeningeal amyloid deposits and ocular manifestations are mainly due to deposits in the viterous[5,6,14,15].

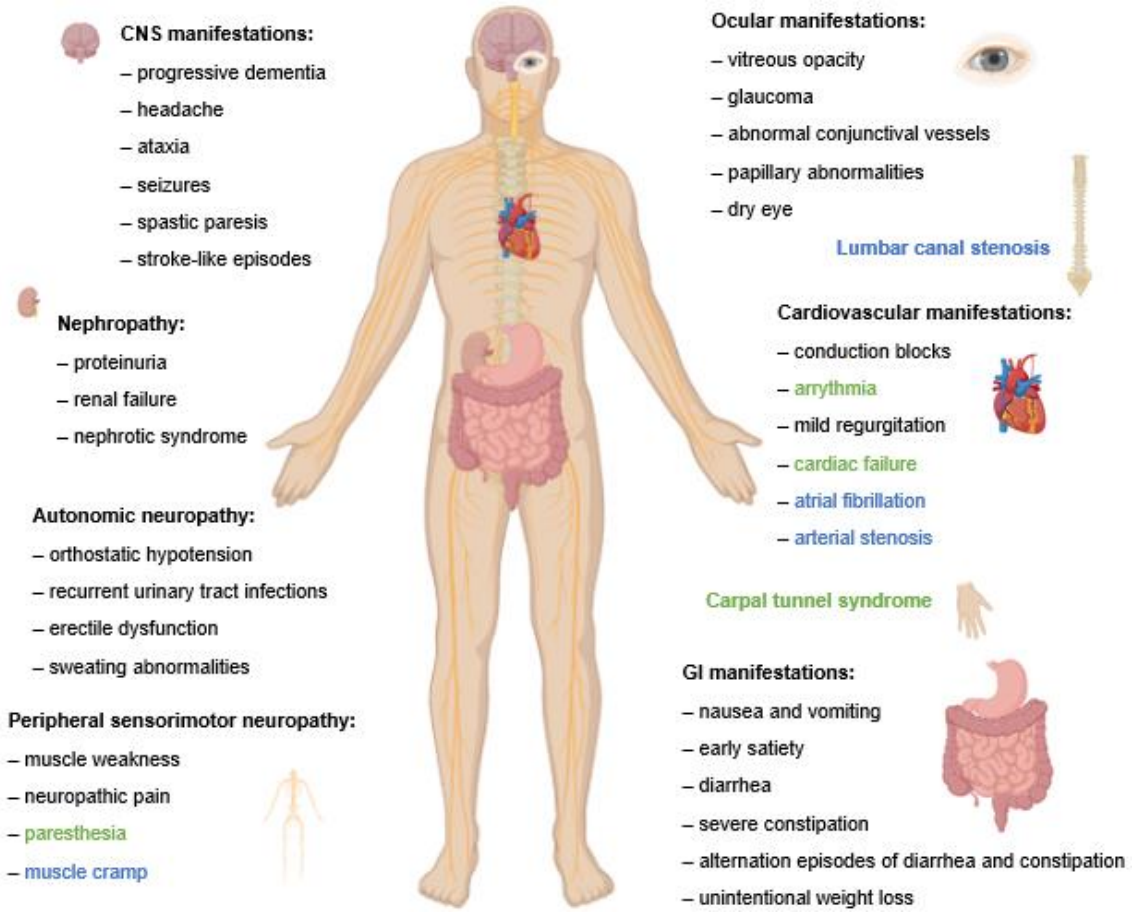

Figure 2 – Clinical features of ATTR amyloidosis. Symptoms only present in ATTRwt amyloidosis are in blue. Symptoms present in both forms of ATTR amyloidosis, ATTRwt and ATTRv are in green[5,14,6,15].

Some clinical manifestations may precede others, Obi and colleagues refer that the carpal tunnel syndrome (which affects 3 to 6% of the general population) may precede cardiomyopathic ATTR amyloidosis in approximately 6 years. Considering the high incidence of the carpal tunnel syndrome, and the advances in non-invasive cardiac diagnostic tools such as cardiac scintigraphy, it is expected an increase of both incidence and prevalence of ATTRwt amyloidosis[7]. Nevertheless, in most people the wild type TTR (TTR wt) deposits are small and probably without clinical significance[4].

2. Transthyretin (TTR)

Transthyretin's designation implies its main function, carrier for both, thyroxine (T4) and retinol (vitamin A), through the retinol binding protein (RBP), so, it stands for **trans**port protein for **thy**roxine and **retin**ol[2].

2.1 TTR structure

Transthyretin (TTR) gene, located on chromosome 18, has four exons, and codes for a polypeptide chain of 127 amino acid and approximately 14 kDa. Four identical peptide chains (monomers) associate forming the native tetrameric form of the protein with an approximate molecular weight of 55 kDa (Figure 3)[1,5,6,16].

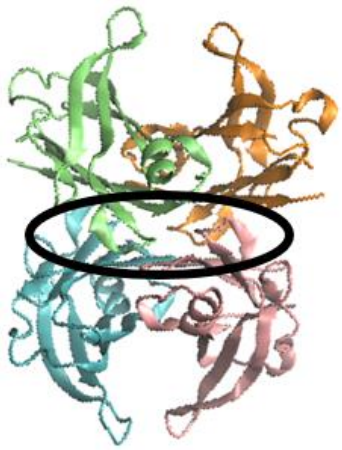

Figure 3 – TTR homotetramer representation using VMD and PDB ID: 4TLT. Each monomer is represented in a different colour and the central hydrophobic channel is signalized.

Each monomer contains 8 antiparallel β-chains and one small α-helix forming two β-sheets[2,17]. Quaternary TTR structure is achieved stepwise, first by association of two monomers through hydrogen bonds, which form a very stable dimer, then, two dimers interact mainly through hydrophobic interactions, forming the TTR homotetramer[2,17].

The homotetramer harbors a central hydrophobic channel (Figure 3) that contains two T4 binding sites at the dimer-dimer interface, and four binding sites at protein surface, two in each dimer, for RBP[2,17].

2.2 TTR metabolism

TTR was first identified in cerebrospinal fluid (CSF) where represents about 25% of the total protein, with a concentration between 5 and 20 mg/l[6]. Later it was detected in human serum, with a concentration around 200-400 mg/l, representing approximately 0,5% of the total protein[6]. It is also present in the aqueous humor of the eyes with a concentration around 5-10 mg/l[6]. TTR concentration is dependent on age, sex, and race, and its levels progressively decline after age of 50 and the age and sex specific differences are eliminated during the age of 70[2,18].

TTR is mainly synthesized in the liver and in the choroid plexus of the brain, but also in the endothelial cells of Islets of Langerhans, ciliary pigment epithelia, retinal pigment epithelium, intestine, visceral yolk sac, and in smaller amounts in the stomach, heart, skeletal muscle and spleen, it is synthesized in the meninges and human placenta[6,19]. TTR expression has also been suggested to occur in Schwann cells, oligodendrocytes, dorsal root ganglia, hippocampal neurons, motor neurons and cerebellar granule cells[6,19].

TTR has a half-life of 1-2 days and is mainly degraded in the liver and kidneys[2]. TTR uptake involves specific receptors, megalin in the kidneys but in the liver the receptor(s) involved is still unknown, nevertheless it is known that is a receptor belonging to low density lipoproteins family sensitive to receptor associated protein[2].

2.3 TTR physiological functions

TTR is mainly recognized as a transport protein, but it also presents proteolytic activity and neuritogenic and neuroprotective roles[1,2,19].

As previously mentioned (section 2.1), TTR possesses two binding sites for T4 but only one molecule of hormone is transported due to negative cooperativity[1]. TTR is responsible for about 15% and 80%, of plasma and CSF T4 transport in humans, respectively[1,6,19]. It was also described as essential for T4 retention in the CSF[1].

TTR possesses four binding sites for RBP, the only specific transport for retinol in circulation[1,19]. Due to these interactions, TTR is responsible, indirectly, for the transport of retinol and, directly, for the retention of RBP in circulation preventing its renal filtration[1,19]. Physiologically, only one of the four binding sites is used for transport; due to steric hindrance, just two RBP molecules may effectively bind to TTR and due to low RBP levels in plasma compared with TTR levels, only one RBP molecule is effectively bound to TTR[4,1].

Other studies found TTR associated with apolipoprotein A-I (apoA-I), and with the nervous system molecules, Aβ peptide and neuropeptide Y (NPY)[1,19]. From these associations new roles were attributed to TTR, namely a neuroprotective role and an enzymatic activity as a zinc dependent metalloprotease[1,19]. TTR is able to cleave apoA-I carboxyl terminal reducing the ability to promote cholesterol efflux[19]. Also, Aβ peptide, aggregated or in its soluble form, was shown to be cleaved by TTR, resulting in decreased Aβ peptide amyloid and toxicity[19]. Furthermore, TTR facilitated Aβ peptide

efflux from the brain and its internalization in the liver via the Lipoprotein-related receptor 1 (LRP-1), showing an effect on Aβ peptide clearance, therefore, in Alzheimer's disease[19]. Though the physiologic relevance of NPY cleavage by TTR is still unknown[19].

Additionally, a neuroprotective role of TTR was also observed in cerebral ischemia, schizophrenia and ALS patients, since TTR levels were decreased[1,19]. Although the TTR molecular mechanisms involved in these neuroprotective roles are not completely known, TTR was described as having a neuritogenic effect in hippocampal neurons, and it was found determinant for hippocampal neuronal survival and neurite outgrowth and preservation[19].

It is clear that TTR is an important gene regulator in CNS[1,19]. In neurons, TTR regulates the expression and interacts with megalin, insulin-like growth factor 1 receptor (IGF1), and δ-γ-aminobutyric acid A receptor (δ-$GABA_A$) which are important molecules involved in neuronal plasticity, synaptic activity, neurite outgrowth and neuronal activity[1,19].

Other TTR ligands have been indicated namely e.g. norepinephrine oxidation products, lutein, pterin, perlecan, lysosome associated membrane protein, metallothionein 2, but the physiologic relevance of these interactions still needs to be elucidated[19].

2.4 TTR variants

As previously mentioned, more than 150 different mutations in the *TTR* gene were described until now, most of them associated with amyloidosis (Figure 4).

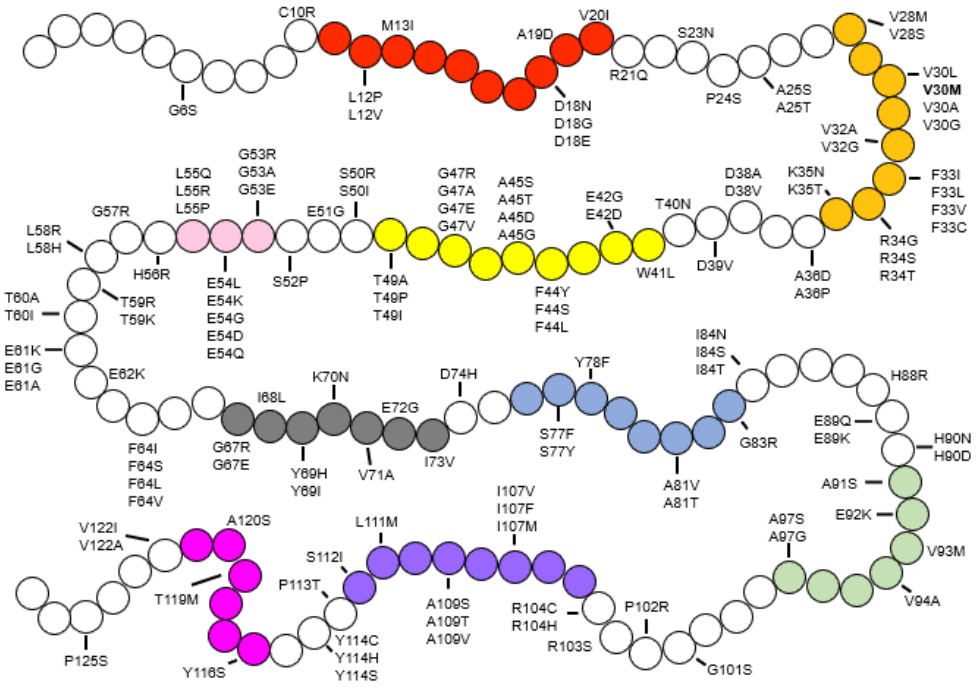

Figure 4 – TTR mutations found in humans. TTR tertiary structure is indicated: β-sheet A. β-sheet B. β-sheet C. β-sheet D. β-sheet E. β-sheet F. β-sheet G. β-sheet H. α-helix. In bold, V30M, the most frequent mutation in the Portuguese population[6,13].

The mutations are distributed in the protein and the analysis of several crystallographic structures revealed small variations in loop regions or local segments around the mutation site, but no major conformational changes except for TTR L55P, which is in accordance with its high amyloidogenic potential[20,21]. These observations indicate that the amyloidogenic propensity is due to TTR tetramer dissociation[20]. Although they present similar crystallographic structures, solution-state nuclear magnetic resonance (NMR) spectroscopy studies revealed differences in the secondary and tertiary structures of two solution structural models of TTR monomeric variants[22].

Overall, TTR monomer instability and/or complex tetramer dissociation pathways seem to be a primary source of TTR pathogenicity, which also lead to different severity of disease, as discussed in the next section[20].

2.5 Amyloid fibril formation

2.5.1 TTR destabilization

The process leading to TTR aggregation and amyloid formation is not fully understood but a key factor for the process is TTR destabilization (Figure 5)[1,17,18,22].

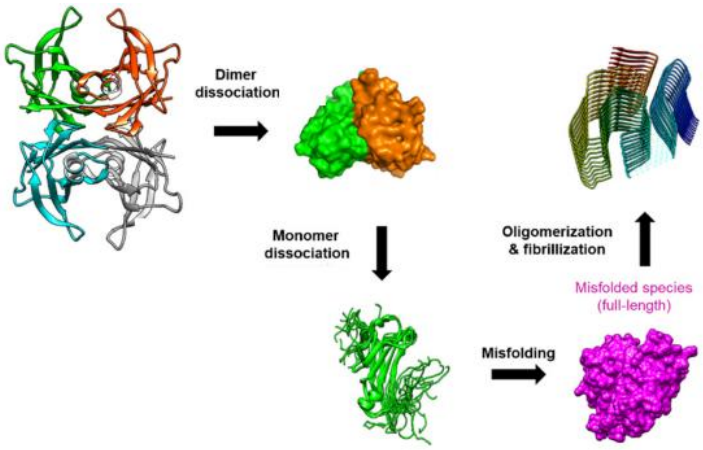

Figure 5 – Suggested TTR destabilization and aggregation mechanism. Adapted from Si et al., 2021[22].

There are biochemical and biophysical evidences suggesting that the TTR homotetramer becomes unstable and dissociates, first into dimers and next into monomers, because interactions between dimers are weaker than the ones between monomers forming the

dimer[1,17,18,22]. Monomers presenting a partially unfolded conformation self-assemble into toxic non-fibrillar aggregates, and after into amyloid fibrils[1].

β-strands C and D were shown to participate in the interchain contacts leading to amyloid formation[23]. And an evolutionary mechanism to decrease proteins' propensity to aggregate is to incorporate gatekeeper residues at the flank of the aggregation-prone segment[23]. In fact, TTR has a lysine in position 35 (K35), in the flank of β-strands C and D, and mutations in this residue also lead to ATTR amyloidosis[23].

TTR tetramer dissociation is strongly influenced by mutations. When analysing TTR V30M, TTR L55P, TTR T119M and TTR V122I dissociation rates it was verified that rapid dissociation increased amyloid formation while slow rates reduced it[24]. TTR T119M is a TTR variant with a very stable tetrameric structure and compound heterozygous ATTR amyloidosis patients carriers of both TTR 119M and TTR V30M show slower progression and mild clinical symptoms when compared with heterozygous patients only with TTR V30M[6]. On the other hand, ATTR amyloidosis patients with TTR L55P present a very early disease age of onset, 15-25 years, which may be due to the fast tetramer destabilization and dissociation (this mutation confers 100% disease penetrance)[24].

In fact, thermodynamic studies suggested that, comparatively to TTR wt, TTR V122I presents a destabilized quaternary structure despite a stable tertiary structure; TTR V30M has stable quaternary structure but unstable tertiary structure; and TTR L55P presents both tertiary and quaternary structures destabilized[20]. Also TTR L55P has a complicated denaturation pathway that includes dimers and trimers as intermediate species[20].

Besides TTR, the amyloid deposits in patients contain other proteins in minor amounts as serum amyloid P component and also proteoglycans[1]. In addition, in the amyloid deposits, the fibrils are composed of full length TTR (type B fibrils) or of a mixture of full length and fragmented TTR (type A fibrils). Type B fibrils were detected in patients with TTR V30M, TTR F64L, TTR D74H and TTR Y114C, and patients with TTR wt amyloid always comprise a mixture of full length and cleaved TTR[1,25,26].

2.5.2 TTR proteolysis

TTR amyloid fibrils from ATTR patients frequently present the TTR 49-127 C-terminal fragment, and in particular in vitreous amyloid deposits[1,2,27]. Amyloid deposits extracted from the heart of cardiac patients revealed that TTR may be cleaved at multiple sites

between the 46 and 52 amino acid residues in polypeptide chain[1,22]. Overall, residues between 46 and 59 were proposed as TTR proteolytic sites[1,22].

The presence of truncated TTR in the amyloid deposits led to propose another mechanism of fibril formation, which involves TTR proteolysis (Figure 6)[1,26].

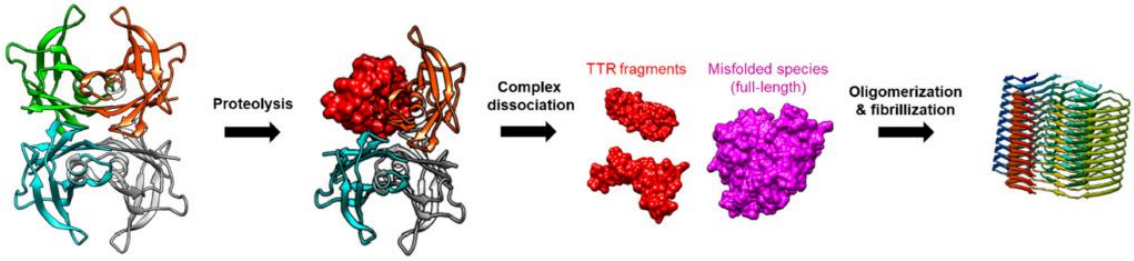

Figure 6 – Suggested TTR proteolysis destabilization and aggregation mechanism. Adapted from Si et al., 2021[22].

Accordingly, one or more monomers in the homotetramer may suffer proteolysis leading to the tetramer destabilization and consequent dissociation. Then, TTR fragments and misfolded monomers (more prone to aggregate) form oligomeric species which precede fibril formation[22].

Regarding this mechanism, some questions remain unanswered, namely whether TTR fragmentation happens before or after aggregation and if it happens in circulation or at the location of deposition[1]. Since plasma from ATTR patients presented higher levels of proteolytic activity as compared with plasma from healthy controls, it was suggested that the process occurs before amyloid fibril formation[1,28].

This has also been considered a mechano-enzymatic mechanism since it considers that shear stress forces of physiological fluid flow, especially in the heart, exposes the protein CD loop that contains a lysine in position 48 (K48), which is then cleaved by a trypsin-like serine protease, namely plasmin, originating TTR 49-127 C-terminal fragment[26,27].

3. Modulators of TTR aggregation

3.1 Small compounds acting as TTR stabilizers

One way to decrease the TTR amyloid propensity is the use of stabilizers, which prevent TTR dissociation into monomers.

Indeed, in clinical practice several small compounds that modulate TTR aggregation are used as tafamidis, diflunisal[2]. Also, some natural compounds were found to stabilize

TTR, as curcumin and epigallocatechin-3-gallate (EGCG), major components of turmeric and green tea, respectively[2].

Tafamidis, diflunisal and curcumin have similar T4 structures and bind to TTR in the T4 binding sites inhibiting its dissociation[2]. EGCG stabilizes TTR through binding at the surface of the TTR molecule, in particular at two biding sites at the dimer-dimer interface exerting an effect similar to a cross linker[2].

Another small compound acting as TTR stabilizer is in phase III clinical trials, acoramidis[2].

3.2 Modulators of the proteolytic activity

TTR fragments identified in the amyloid deposits as TTR 49-127 C-terminal or TTR 81-127 C-terminal are consistent with a trypsin-like serine protease like plasmin[1,29,30]. Plasmin is an ubiquitously distributed serine protease, unlike trypsin that is exclusively located in duodenum[1,29,31].

Plasmin is continuously activated by cleavage of plasminogen, and is essential for fibrin enzymatic degradation in blood clots preventing the obstruction of blood vessels and in the extracellular matrix (fibrinolysis), it maintains homeostasis[29,31,32]. Additionally, it has other functions unrelated to fibrin removal[32]. Plasminogen is mainly synthesized in the liver and is found in plasma at concentration around 180 µg/ml with a plasma half-life around 2 days[31,32].

Plasmin is involved in wound healing and tissue repair, bone healing and remodelling, harnessed by pathogens (infectivity/avoid host immunity), angiogenesis and metastases, skin pigmentation, immunity and inflammation and also in clearance of cellular debris and misfolded/aggregated proteins[1,32]. Moreover, activation of plasminogen activation system (PAS) was described in Alzheimer's disease and in immunoglobulin light chain amyloidosis, both amyloid related diseases[32]. Plasmin was also involved in TTR amyloidosis, since it triggers amyloid formation *in vitro* and promotes amyloid deposition in a mouse transgenic model[29,30].

As previously mentioned, plasmin is a serine protease and it is tightly regulated by α-2-antiplasmin, or SerpinF2, but not only[31,32]. These could act as proteolysis modulators.

Serine **p**rotease **in**hibitors (Serpins) are a superfamily of proteins identified in all five kingdoms, their structure is characterized by a core domain with three β-strands, 8 or 9

α-helices and a centrally located reactive centre loop (RCL) with approximately 17 residues long[33,34].

The target substrate (protease) is defined by the RCL and its effectiveness of inhibition also depends on protein flexibility [33,34].

Serpins establish a covalent ester bond with the protease, consequently changing their target and inhibiting its function, in a mechanism named "suicide substrate inhibition"[33]. The interactions that follow are the same as those that take place during a typical protease catalysis[33].

Serpins are grouped into clades according to their sequence similarity, humans harbour 36 protein coding genes whereas mice have 60[33,35].

Indeed, SerpinA1 (α-1-antitrypsin) and SerpinA3 (α-1-antichymotrypsin) levels were altered in serum from TTR V30M patients and in serum associated with polyneuropathy, respectively[28,36]. Using a differential proteomics approach, SerpinA1 was found overrepresented in ATTR amyloidosis patients heterozygous for TTR V30M[28]. On the other hand, SerpinA3 plasma protein levels were decreased in FAP when compared with FAC patients or with healthy controls, although no differences were observed for FAC patients when compared with healthy controls[36].

SerpinA1 is mainly synthesized in the liver, but also in the lungs and intestine, neutrophils, macrophages, and cornea, its main function is to protect lung tissue by inhibiting cathepsin G, serine proteases neutrophil elastase and proteinase 3[35,37]. It is involved in inflammation, complement activation, apoptosis[35,37]. It is found in plasma at concentration about 1-2 mg/ml[38].

SerpinA3 is mainly synthesized in the retina, kidneys, liver and pancreas[33]. It is involved in inflammation, complement activation, apoptosis, prohormone conversion, Alzheimer's disease[33,35]. In Alzheimer's disease studies suggest that it mediates Aβ peptide clearance, but its main function is to counterbalance inflammation due to interaction with cathepsin G[33,34].

Serpina3n is the mouse ortholog of human SerpinA3. The RCL sequence of Serpin3n is identical to human SerpinA1 and shares a 61% homology with SerpinA3 (excluding RCL)[34]. It has overlapping function with both SerpinA1 and SerpinA3 and exhibits a diversity of target substrates[34].

Aims

Cardiomyopathy is the most frequent ATTR amyloidosis phenotype related to TTR wt and TTR V122I, one of the most frequent TTR variants world wide, and, although the molecular mechanisms involved in the fibril formation still need more investigation, TTR proteolysis emerged as a relevant contribution in the process. Furthermore, plasmin was shown to be a potential protease involved in TTR cleavage[29,30]. In addition, some studies showed that specific Serpins levels were altered in ATTR amyloidosis patients, namely SerpinA1 and SerpinA3[28,36].

Also, studies in HM30 mice (knockout for mouse *ttr* gene and transgenic for human *TTR* V30M gene) treated with oncostatin M revealed an increase of Serpina3n in their liver accompanied by a decrease of TTR expression and protein levels, as well as an increase of Serpina3n expression levels in their heart (unpublished data from our group, Molecular Neurobiology Group, IBMC, i3S).

Therefore, aiming to contribute to the knowledge of relevance of proteolysis in amyloidosis pathogeny and the associated molecular mechanisms we established the following objectives:

- to characterize HM30 mice regarding Serpina3n levels and compare them to control mice (WT mice not transgenic for *TTR* gene);
- to establish a primary cardiomyocyte cell culture to be used for the cellular studies with different TTR aggregates;
- to characterize TTR wt aggregation under proteolytic conditions;
- to elucidate the effect of TTR wt aggregates formed under proteolysis in the HL-1 cardiomyocyte cell line;
- to characterize TTR wt, TTR L55P, TTR V122I and TTR fragment 49-127 aggregation not submitted to proteolysis;
- to elucidate the molecular mechanisms involved in the cellular response to TTR wt, TTR L55P, TTR V122I and TTR fragment 49-127 aggregates (not submitted to proteolysis) in the HL-1 cardiomyocyte cell line.

Material and Methods

1. Biological samples

Mice tissues, liver and heart, and also plasma were already available at the laboratory. Even if not performed directly under the scope of this project all animal experiments were approved by the Portuguese General Veterinarian Board (authorization number 014982 from DGV-Portugal) and animals were kept and used strictly in accordance with National rules and the European Communities Council Directive (86/609/EEC), for the care and handling of laboratory animals.

The mice strains used were wild type mice (IW) and HM30 mice. HM30 mice are transgenic for human *TTR* gene, with the point mutation originating V30M substitution, and knockout for mouse *ttr*[39]. The samples were stored at – 80 °C. In some cases, the tissue homogenates were already available, otherwise they were prepared. For mRNA extraction, tissues were homogenized with TRIzol® Reagent and total RNA was isolated according to the manufacturer's instructions. For protein extraction, tissues were homogenized using RIPA lysis and extraction buffer according to the manufacturer's instructions (Santa Cruz Biotechnology, Dallas, TX, USA). Relative concentrations of Serpina3n were evaluated by western blot analysis.

2. Quantitative Real-Time PCR (qRT-PCR) of Serpina3n

Total RNA from heart and liver tissues was extracted with TRIzol® Reagent (Thermo Fisher Scientific™, Rockford, IL, USA). Briefly, tissues were homogenized with 1 ml Trizol and incubated for 5 minutes at room temperature (RT). Then, 200 µl of chloroform were added, and the samples were incubated under shaking for 3 minutes at RT. The homogenates were centrifuged at 8000 rpm for 15 minutes at 4 °C, the upper phase was removed, and 500 µl of isopropanol were added to the lower phase. Tubes were mixed by inversion, incubated for 10 minutes at RT, and centrifuged at 9000 rpm for 10 minutes at 4 °C. The resulting pellet was washed with 1 ml 75% ethanol and centrifuged again at 5000 rpm for 5 minutes at 4 °C. The supernatant was discarded and the RNA pellet was dried. The pellet was dissolved and homogenized in pure water (50 to 100 µl) and incubated at RT for 10 minutes. Afterwards, samples were incubated for 7 minutes at 57 °C and RNA was quantified using the *NanoDrop™ One* Microvolume UV-Vis

Spectrophotometer (Thermo Scientific™, Rockford, IL, USA) and frozen at – 80 °C. RNA quality was assessed by Experion™ Automated Electrophoresis Station (Bio-Rad, Hercules, CA, USA). Only RNA preparations with RNA quality indicator (RQI) higher than six were used for further analyses. Each sample was reverse transcribed using 1 µg of RNA, random hexamers or oligodT (for liver or heart RNA, respectively) and the SuperScript® First-Strand Synthesis System for RT-PCR (Invitrogen, Carlsbad, CA, USA) according to the suppliers' instructions in a T100™ Thermal Cycler (Bio-Rad, Hercules, CA, USA). Relative quantification of Serpina3n mRNA was performed using 40 cycles at 55° in a CFX96 Touch Real-Time PCR Detection System (Bio-Rad, Hercules, CA, USA) using iTaq Universal SYBR® Green Supermix (Bio-Rad, Hercules, CA, USA) and specific primers (Sigma-Aldrich, St. Louis, MO, EUA) described in Table 1. Serpina3n mRNA levels were normalized to Gapdh or 18S content, for heart or liver, respectively, using CFX Maestro software (Bio-Rad, Hercules, CA, USA).

Table 1 – Primer sequences used in qRT-PCR analysis.

Gene	Sequence (5' to 3')
Serpina3n (sense)	TGGTGCTGGTGAATTATATC
Serpina3n (antisense)	GCGTAGAACTCAGACTTG
Gapdh (sense)	GCCTTCCGTGTTCCTACC
Gapdh (antisense)	AGAGTGGGAGTTGCTGTTG
18S (sense)	ACAGGATTGACAGATTGA
18S (antisense)	TATCGGAATTAACCAGACA

3. Recombinant protein production

Recombinant TTR wt was produced using an *E. coli* bacterial expression system described by Furuya et al., 1991[40]. It follows a brief description. All procedures were performed in sterile conditions.

3.1 Transformation

The BL21 (DE3) *E. coli* competent cells, thawed on ice, were transformed with 50 to 100 ng of pINTR WT plasmid DNA, on a 13 ml tube, and maintained on ice for 30 minutes. The cells were then submitted to a thermal shock at 42 °C for 45 seconds, followed by incubation on ice for 2 minutes. Then, 100 µl of Luria-Bertani (LB) medium were added to the transformed cells, under the flame, and the solution was incubated at 37 °C, under

shacking for 1 hour. Two aliquots of 10 and 90 µl of the culture were plated on LB-agar-ampicillin plates (LB-agar-ampicillin plates contained 15 g/l of agar in LB medium, and 0.1 mg/ml of ampicillin). The plates were incubated overnight at 37 °C and on the following day were stored at 4 °C.

3.2 Bacterial culture – protein production

First, a pre-culture was prepared in an Erlenmeyer with 100 ml of LB medium with ampicillin (0,1 mg/ml) that were inoculated with a single colony of *E. coli* transformed with pINTR WT. The culture was incubated overnight, under shacking, at 37 °C. Then, the pre-culture was used to inoculate a new bacterial culture grown in M9CA medium (1×) supplemented with calcium chloride (0,1 mM), ampicillin (0,05 mg/ml), magnesium sulphate (2 mM), and glucose (0,2 %) at 37 °C, under shacking until the optical density (Genesys 10 Bio spectrophotometer, Thermo Scientific, Rockford, IL, USA) at 600 nm ($O.D._{600nm}$) reached 0,5-0,6 (exponential growth). The bacterial culture growth was monitored every 30 minutes. Aliquots of 1 ml were harvested and stored at 4 °C for analysis. Then the expression of the protein was induced with 0,15 mM isopropyl β-D-thiogalactopyranoside (IPTG) (Thermo Scientific, Rockford, IL, USA) and the culture was incubated overnight, under shacking, at 30°C. On the next day, another aliquot was harvested. All the aliquots were stored at frozen at – 20 ºC for posterior analysis.

3.3 Osmotic shock

TTR was recovered from the bacterial periplasm by osmotic shock. The bacterial culture was divided into centrifuge flasks, and centrifuged (High Speed Centrifuge Beckman Avanti J-26 XP, Beckman Coulter Life Sciences) at 4 000 rpm, for 15 minutes at 4 °C. The supernatant was discarded, and the bacterial pellet resuspended in 20% saccharose in 50 mM Tris pH 7,5, containing 0,5 mM EDTA solution. The suspension was incubated at RT, under shacking, for 10 minutes and was centrifuged, at 4000 rpm for 40 minutes, at 4 °C. The supernatant was discarded, and the pellet was resuspended in an ice-cold solution of 50 mM Tris pH 7,5 and incubated on ice, under shacking, for 10 minutes. A last centrifugation at 4000 rpm for 50 minutes, at 4 °C allowed the removal of bacterial debris. The supernatant containing the recombinant TTR was collected and stored at – 20 °C.

Periplasm bacterial proteins were fractionated by ion exchange chromatography using Nuvia Q (Bio-Rad, Hercules, CA, USA) or diethylaminoethyl cellulose (DEAE, Whatman, Maidstone, UK) as ion exchange resins, and elution with increasing concentration of sodium chloride (NaCl). The resin was equilibrated overnight at room temperature with 50Mm Tris pH 7,5 and transferred to the chromatography column. When the resin was settled, the result of the osmotic shock flowed through it and the protein elution started with step salt increase NaCl/50mM Tris pH 7,5 (0,1 M NaCl to 0,5 M NaCl). The elution of protein was monitored by measurement of absorbance at 280 nm. TTR was mainly eluted with 0,3 M NaCl with Nuvia Q and with 0,2 M NaCl with DEAE. The preparations obtained were analysed by electrophoresis in 15% polyacrylamide gel with sodium dodecyl sulphate (SDS-PAGE) analysis.

3.4 Protein purification by chromatography and electrophoresis

Ultrafiltration units (Vivaspin, GE Healthcare, Chicago, IL, USA) were used to concentrate protein samples and to dialyze them (according to the manufacturer's instructions). Briefly, protein was concentrated by centrifugation in the ultrafiltration units followed by three exchange buffer cycles using 50 mM Tris pH 7,5 buffer.

The protein was separated by electrophoresis in a metaphor agarose gel (4 %), the TTR band was excised from the gel and electroeluted.

Proteins to be used in cell culture were detoxified using a Detoxi-Gel™ Endotoxin Removing Gel (Thermo Fisher Scientific™, Rockford, IL, USA) to eliminate possible contaminations with bacterial lipopolysaccharides according to the manufacturer's instructions. Protein was stored at – 20 °C with DPBS (Dulbecco's Phosphate Buffered Saline, Sigma-Aldrich, St. Louis, MO, EUA).

4. Protein aggregation studies

4.1 Aggregation in proteolytic conditions

Recombinant human TTR wt (Alexotech, Umeå, Sweden) was solubilized in phosphate buffered saline buffer (PBS, pH 7,4, Lonza, Basel, Switzerland) and filtered through a sterile 0,2 µm inorganic membrane ANOTOP syringe filter (Whatman, Maidstone, UK) to remove any protein aggregates if existing. Filtered TTR (18 µM) was incubated with native human plasmin protein (active) (0,4 U, abcam, Cambridge, UK) and/or native human SerpinA1 protein (active) (2,8 µM, abcam, Cambridge, UK), or alone, for 24 hours

at 37 °C. Proteolysis was ceased by addition of 1,5 mM phenylmethanesulfonyl fluoride (PMSF, Sigma-Aldrich, St. Louis, MO, USA).

4.2 Aggregation without proteolysis

Recombinant human TTR wt and variants, TTR L55P, TTR V122I and TTR fragment 49-127 (Alexotech, Umeå, Sweden) were solubilized in filtered and sterile PBS pH 7,4. The protein solutions (18 μM) were incubated for 0 or 48 hours at 37 °C. Additionally, samples of TTR wt and TTR L55P were incubated for 120 hours at 37 °C.

5. Analysis of aggregated samples

Protein samples from aggregation assays were analysed by Thioflavin T (ThT), Dynamic light scattering (DLS) and/or Transmission electron microscopy (TEM).

5.1 Thioflavin T (ThT) assay

Thioflavin T assay was performed in PBS (pH 7,4) using a 96 well black bottom plate. Protein samples from the aggregation assays (TTR, 12,5 μg) were mixed with ThT solution (30 μM) (Sigma-Merck, Darmstadt, Germany) in each well and the fluorescence at 25 °C was measured under excitation and emission wavelengths of 450 and 482 nm, respectively, using a SynergyMx apparatus (BioTek, Winooski, VT, USA).

5.2 Dynamic Light Scattering (DLS)

Dynamic light scattering (DLS) measurements were performed at 25 °C using a Marvern Zetasizer Nano ZS device (Malvern, Worcestershire, UK). Protein samples from aggregation assays (50 μl) were measured three times and size distributions by intensity were determined using laser detection angle of 173° and 12,8°. DLS (nano) software (Malvern Instruments) represented the results as figures, “Size Distribution by Intensity”.

5.3 Transmission Electron Microscopy (TEM)

Aliquots of 5,0 μl of different TTR aggregation samples were withdrawn at different incubation times, loaded onto a formvar/carbon-coated 400 mesh copper grids for

electron microscopy (Agar Scientific, Stansted, UK) and negatively stained with 1,0% (w/v) uranyl acetate (Electron Microscopy Sciences, Hatfield, PA, USA). The grid was air-dried and examined using a transmission electron microscope JEM 1400 (JEOL, Welwyn Garden City, UK) at 80kV accelerating voltage.

6. Cell culture assays

6.1 Preparation of primary culture of mice cardiomyocytes

Primary cardiomyocyte (PC) cells were obtained using Pierce™ Primary Cardyomyocyte Isolation Kit (Thermo Scientific, IL, USA) according to the instructions of the manufacturer. Briefly, mice pups (one day old) were anaesthetized, and their heart extracted. Hearts were introduced into 1,5 ml sterile microcentrifuge tubes with ice cold Hanks' Balanced Salt Solution (HBSS, Thermo Scientific, IL, USA), cut into 3-4 pieces and washed twice with ice cold HBSS. The tissue was digested for 35 minutes at 37 °C with Cardiomyocyte Isolation Enzyme 1 and 2 (Thermo Scientific, IL, USA) with papain and thermolysin, respectively. After two washes with ice cold HBSS, Complete Dulbecco's Modified Eagle's Medium (DMEM, Thermo Scientific, IL, USA) for Primary Cell Isolation was used and heart tissue was broken up by pipetting up and down. Individual cell suspensions were combined, and cell yield and viability were determined. For the cell culture, a seeding density of $2{,}5\times10^5$ cells/cm^2 was used in 6 well plates. The cells were incubated for 24 hours in a cell culture incubator at 37 °C (with 5% CO_2). Then the medium was replaced with Complete DMEM for Primary Cell Isolation containing Cardiomyocyte Supplement (1 ‰). The culture was maintained by changing the medium every 3 days. At days 4 and 7 protein markers (cardiac troponin T and vimentin) were analysed by western blot.

6.2 Cell culture of HL-1 cardiomyocytes

Immortalized mouse cardiomyocyte cell line (HL-1), kindly provided by doctor Perpétua Pinto do Ó (Instituto Nacional de Engenharia Biomédica, INEB, i3S) was maintained in Claycomb basal medium (Sigma-Merck, Darmstadt, Germany), supplemented with HL-1 screened fetal bovine serum (FBS, 10% (v/v), Sigma-Merck, Darmstadt, Germany), penicillin/streptomycin (1% (v/v), Sigma-Merck, Darmstadt, Germany), L-glutamine (2mM, Sigma-Merck, Darmstadt, Germany) and (+)-norepinephrine [(+)-arterenol] (0.1mM, Sigma-Merck, Darmstadt, Germany) in the cell culture incubator.

6.2.1 Cell viability assays

HL-1 cardiomyocytes' cytotoxicity assays were performed using a 96 well with Lid Black with Clear Flat Bottom, Tissue Culture Treated Polystyrene Non-Pyrogenic plate. The cells were let to adhere for more than 24 hours and the assays were performed with a cell confluency around 90%. The different protein preparations (at 2 μM concentration) were added to each well in Claycomb serum free medium for 3 and/or 24 hours in a cell culture incubator at 37 °C. Following, 20 μl of Resazurin solution Assay Kit – Cell Cytotoxicity (Fluorometric) (Abcam, Cambridge, UK) were added to each well and incubated for one hour at 37 °C. Viability was assessed by measurement of fluorescence under excitation and emission wavelengths of 540 and 590 nm, respectively, using SynergyMx apparatus. Controls were also performed, control without cells, vehicle control (filtered and sterile PBS, pH 7,4), and positive control incubation with saponin (25 μg/ml/well, Sigma-Merck, Darmstadt, Germany).

6.2.2 Apoptosis through caspase 3/7 activity assay

HL-1 cardiomyocytes' caspase 3/7 activity assay was performed using a 96 well white/clear bottom plates. Assays were performed with a cell confluency around 90%, cells were let to adhere for more than 24 hours. Then, the cells were incubated with 2 μM of the different protein preparations in Claycomb serum free medium for 3 and 24 hours in cell culture incubator at 37 °C. Afterwards, in each well, 100 μl of Caspase-Glo® 3/7 Assay (Promega, Madison, WI, USA) reagent were added and plates were equilibrated at RT for 30 minutes. Apoptosis was assessed by measurement of luminescence using SynergyMx apparatus. We performed control without cells, vehicle control (PBS), and positive control incubation with staurosporine (1 μM/well, Sigma-Merck, Darmstadt, Germany).

6.2.3 Analysis of biomarkers by Western blot

We performed western blot analysis of protein samples from different assays, namely liver and heart tissue homogenates and plasma from mice, primary cardiomyocytes and HL-1 cardiomyocytes.

RIPA Lysis Buffer System (ChemCruz, Dallas, TX, USA) was used to extract protein content from tissue homogenates, primary cardiomyocytes and HL-1cells. Total protein was quantified using Protein Assay Dye Reagent Concentrated (BioRad, Hercules, CA,

USA). For the electrophoresis, 25 to 50 µg of protein were separated in 12 or 15% polyacrylamide gels (SDS-PAGE). The plasma samples were diluted and 5 µg of total protein were analysed in the 12% SDS-PAGE. Proteins were electrically transferred to Amersham™ Protran™ 0.2 µm NC Nitrocelulose Blotting Membrane (GE Healthcare Live Science, Taufkirchen, Germany) followed by membrane blocking for 1 hour at RT with 5% non-fat dried milk in PBST (PBS-Tween20) or 5% bovine serum albumin (BSA) in PBST.

Membranes were blocked with primary antibodies listed in Table 2, for 1 hour at RT or overnight at 4 °C.

Table 2 – Primary antibodies used in western blot analysis.

Antibody	Dilution	Supplier
rabbit anti-human prealbumin (Transthyretin) (Multipurpose)	1:1000	Dako, Hovedstaden, Denmark
mouse anti-transthyretin mutant (Y78F), clone AD7	1:100	Sigma-Merck, Darmstadt, Germany
rabbit anti-mouse Fas	1:500	Santa Cruz Biotechnology, Dallas, TX, USA
rabbit anti-mouse Grp78/BiP	1:1000	abcam, Cambridge, UK
rabbit anti-mouse BMP-10	1:1000	Biorbyt, Cambridge, UK
rabbit anti-mouse cTnT	1:250 (HL-1 cells) 1:1000 (PC)	Invitrogen, Rockford, IL, USA
rabbit anti-mouse vimentin	1:1000	Cell Signalling, Danvers, MA, USA
rabbit anti-mouse LC3A/B	1:500	Cell Signalling, Danvers, MA, USA
mouse anti-human SQSTM1/p62	1:1000	abcam, Cambridge, UK
rabbit anti-mouse GAPDH	1:100000	abcam, Cambridge, UK
mouse anti-β-actin antibody	1:5000	abcam, Cambridge, UK
goat anti-Serpina3n antibody	1:500	Thermo Fisher scientific, Waltham, MA, EUA

Detection was achieved using Horseradish Peroxidase (HRP) conjugate, cross-adsorbed secondary antibodies listed in Table 3 (incubation for 35 minutes) and visualized with Clarity™ Western ECL Substrate (BioRad, Hercules, CA, USA). After

each antibody incubation, membranes were washed three times for 10 minutes with PBST. Immunoblot quantitative analysis was performed using Image Lab software (BioRad, Hercules, CA, USA).

Table 3 – Secondary antibodies used in western blot analysis.

Antibody	Dilution	Supplier
goat anti-mouse IgG (H+L)	1:5000	ThermoFisher Scientific, Rockford, IL, USA
donkey anti-goat IgG (H+L)	1:5000	Invitrogen, Frederick, MD, USA
goat anti-rabbit IgG (H+L)	1:5000	Invitrogen, Frederick, MD, USA

7 Statistical analysis

Statistical analysis was performed by one-way ANOVA (Tukey's multiple comparisons as post-test) or Students t-test (Mann-Whitney U test) using GraphPad Prism 8.0.2 software (San Diego, CA, USA). Statistical significance was considered when p-value <0,05. Results were expressed as mean ± standard error of the mean (SEM).

Results and Discussion

Part A – Serpina3n analysis in HM30 mice

SerpinA3 is known to be associated with inflammation, and its levels were decreased in ATTRv patients' serum associated with polyneuropathy[34,36]. Also, studies in HM30 mice treated with oncostatin M revealed an increase of Serpina3n in their liver accompanied by a decrease of TTR expression and protein levels, as well as an increase of Serpina3n expression levels in their heart (unpublished results from the lab).

We first evaluated Serpina3n expression levels in the liver and heart of HM30 mice group (n=5) by qRT-PCR analysis and compared with the levels for WT mice group (n=4) of 12-15 months of age (Figure 7). As references we used 18S ribosomal RNA for liver and gapdh mRNA for the heart.

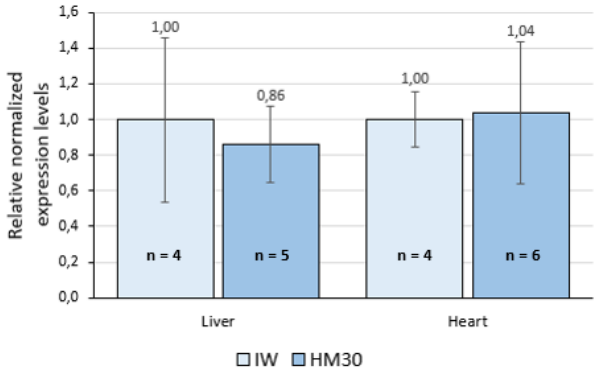

Figure 7 – Serpina3n relative mRNA levels in the liver and heart of HM30 and IW mice. qRT-PCR analysis of mRNA levels relative to 18S ribosomal RNA and gapdh, for liver and heart, respectively. Wild type mice (IW) levels were used to normalize. Statistical analysis was performed using t-test.

The results obtained show that at 12-15 months of age Serpina3n mRNA levels are similar for both mice groups, IW and HM30 mice, independently of tissue (liver or heart).

After, we evaluated Serpina3n relative protein levels, by western blot, in the liver, heart and plasma in the same groups of mice (Figure 8).

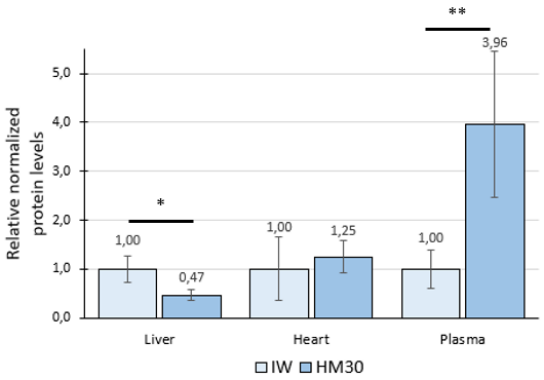

Figure 8 – Serpina3n relative protein levels in the liver, heart and plasma of HM30 and IW mice. β-actin and GAPDH were used as loading controls for liver and heart samples, respectively. For plasma, one control sample was used in all immunoblots. IW mice levels were used to normalize Serpina3n. Data from three WB analysis, expressed as mean ± SEM. IW (n=6), HM30 (n=11). Statistical analysis was performed using t-test. * p<0,05, ** p<0,01.

Liver's Serpina3n protein levels were lower for HM30 mice than for IW mice. On the contrary, Serpina3n plasma levels are higher for HM30 mice than for IW mice, reaching statistical significance. No differences were observed in the heart.

Several tissues express Serpina3n, but this protein is mainly synthetized by hepatocytes.[34,41] Our results indicate that, in the liver, despite similar mRNA expression levels were found among IW and HM30 groups, lower Serpina3n concentration was found in the liver of HM30 mice group. This might indicate that more protein is secreted to the plasma and this is in accordance with the higher concentration of Serpina3n found in the plasma of HM30 mice.

We hypothesize that SerpinA3 could be acting as a molecular chaperone and as such being recruited to interact with TTR in plasma inhibiting aggregation and fibril formation. Increased Serpina3n protein levels in circulation may also play a role in preventing TTR proteolysis and aggregation and fibrils formation to contradict deposition in tissues in HM30 mice. In future studies, groups of mice of different ages, either younger (4-6 months) and older (18-24 months) should also be investigated.

Part B – TTR aggregation studies

1. Recombinant TTR wt production and purification

The protocol to express recombinant TTR wt in *E. coli* was already well stablished in our laboratory. TTR wt was produced in BL21 (DE3) *E. coli* competent cells using the vector pINTR WT and, to separate human TTR wt from bacterial proteins obtained after the osmotic shock, an ion exchange chromatography was used. We tested two different ion exchange resins, Nuvia Q (Figure 9) and DEAE-cellulose (Figure 10).

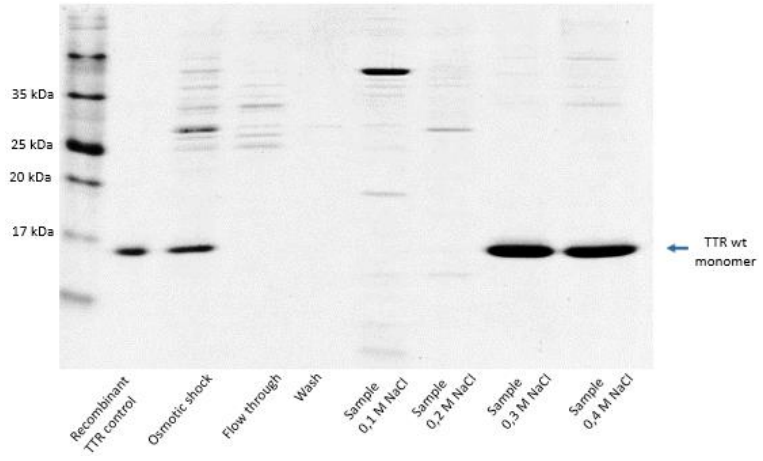

Figure 9 – Analysis of fractions from different steps of the purification of recombinant TTR wt using Nuvia Q. SDS-PAGE stained with Coomassie blue. Molecular weights are referred to the protein ladder.

The results obtained for the chromatography with Nuvia Q demonstrate that TTR was mainly eluted with 0,3 NaCl in 50 mM Tris in fractions with minor contaminations by other proteins. TTR was also eluted with 0,4 M NaCl in 50 mM Tris though, these fractions presented higher contamination with other proteins. It was also possible to verify that TTR was not present in the solution eluted from the column without salt (flow through and wash).

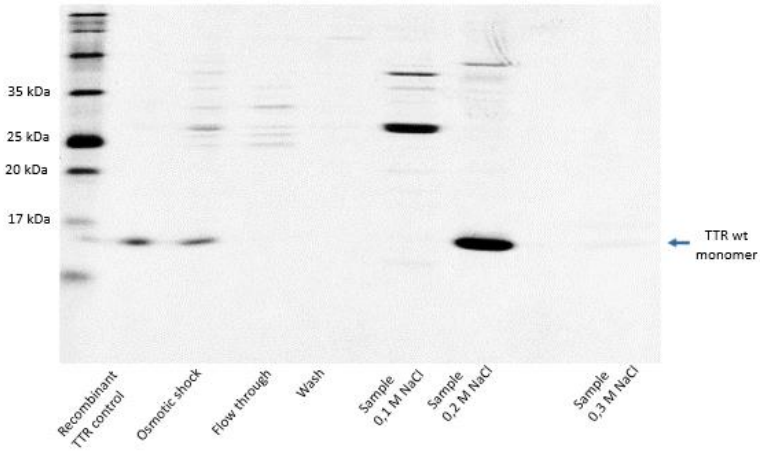

Figure 10 – Analysis of fractions from different steps of the purification of recombinant TTR wt using DEAE-cellulose. SDS-PAGE stained with Coomassie blue. Molecular weights are referred to the protein ladder.

When using DEAE-cellulose, TTR was eluted with 0,2 M NaCl in 50 mM Tris fractions with minor protein contaminations, but when compared with Nuvia Q resin, more contaminants were observed. Similarly to the previous chromatography, no TTR was lost in the flowthrough and wash fractions from the column without salt.

For the subsequent separations we used Nuvia Q resin due to less amount of contaminant proteins. But since we obtained contaminations, we proceeded with purification in an agarose metaphor gel electrophoresis and electroelution which allowed us to obtain pure TTR wt protein (Figure 11).

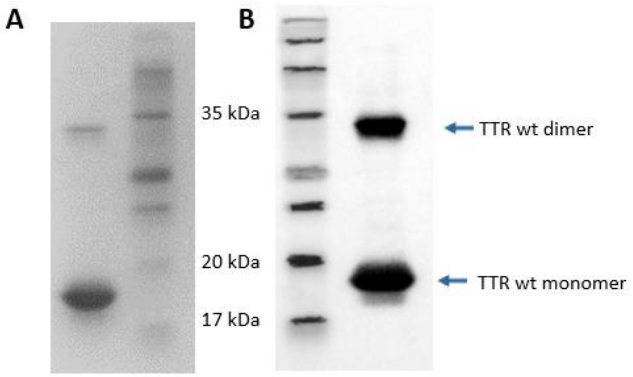

Figure 11 – Recombinant TTR wt obtained after electroelution. **A:** SDS-PAGE stained with Coomassie blue. **B:** Western blot analysis with antibody against human TTR. Molecular weights are referred to the protein ladder.

We successfully produced, purified and removed endotoxins with a column with Detoxi-Gel^{TM} endotoxin removing gel so that recombinant TTR wt without bacterial lipopolysaccharides could be used in cellular studies.

2. Establishment of primary mice cardiomyocytes culture

We performed preliminary studies with neonatal (one day old pups) mice cardiomyocytes to establish a primary cardiomyocytes culture. We successfully collected and maintained primary cardiomyocytes from neonatal B6 mice (wild type) for 7 days.

We observed a more frequent and vigorous contraction of primary cardiomyocytes at day 4 than at day 7.

We tested cardiomyocytes viability by their ability to express cardiac Troponin T (cTnT) and vimentin (Figure 12). We used cTnT because it is a highly specific and sensitive marker for myocardial injury[42]. Cardiac troponins are predominantly structurally bound

within the thin filaments of the contractile apparatus and are released to circulation after cardiac damage and ultimately, cardiac necrosis, studies found that loss of cTnT in the tissue may precede histologic evidence of cardiac necrosis[43]. Vimentin was chosen because although it is not expressed in cardiomyocytes, it is expressed in fibroblasts, vascular endothelial and smooth muscle cells that should also be present in our preparation[44,45,46].

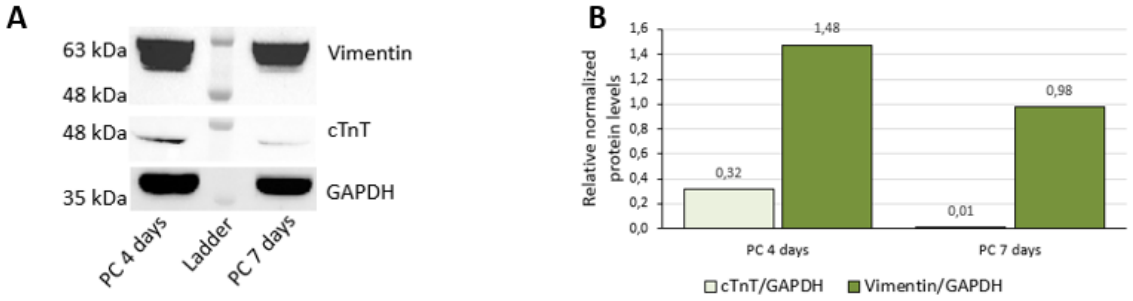

Figure 12 – Protein markers of myocardial injury. **A:** Western blot analysis, cTnT and vimentin were analysed in primary cardiomyocytes (PC) at 4 and 7 culture days. **B:** cTnT and vimentin protein levels were normalized to loading control GAPDH. Molecular weights referred to the protein ladder.

After 7 days in culture, cells lost their ability to express cTnT and decrease vimentin indicating cellular damage, reason why we observed a decrease in cellular contraction. Therefore, in future assays we shall maintain our culture for no more than four days.

Primary cardiomyocytes culture had as disadvantages the reduced cell number obtained in the procedure, as well as the low recommended cell density per well, which may be limiting for protein detection by immunoblotting.

We proceeded our TTR aggregation cellular studies with the HL-1 cardiomyocytes cell line. Nevertheless, we shall optimize conditions to use primary cardiomyocytes in cellular studies, because it will be better to complement results using a nonimmortalized cell culture.

3. TTR aggregated samples in proteolytic conditions

To study TTR wt aggregation under proteolytic conditions we used recombinant TTR wt commercially available. Wild type TTR was incubated at 37ºC for 24 hours in the presence of plasmin (proteolytic conditions) or in its absence (no proteolytic conditions). In addition, similar samples were prepared in the presence of SerpinA1, or in its absence.

Aggregation was evaluated through measurement of fluorescence upon addition of ThT (Figure 13).

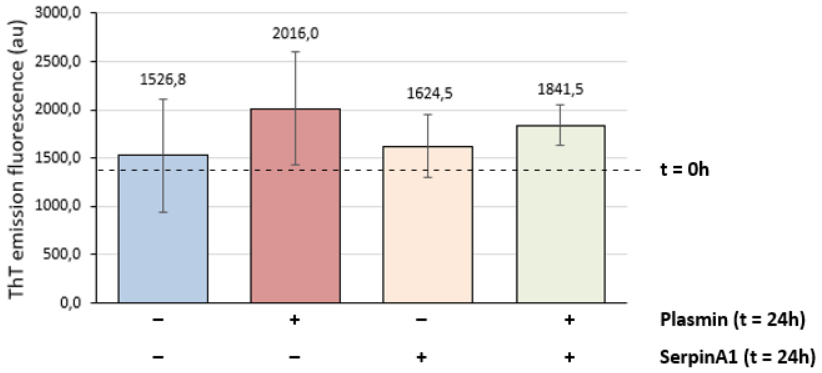

Figure 13 – Modulation of TTR wt aggregation by plasmin and SerpinA1. Aggregation was evaluated by ThT emission fluorescence. TTR was incubated in the presence and/or absence of plasmin and/or SerpinA1, for 24 hours at 37 °C. Data from two (n=2) independent in vitro experiments, expressed as mean ± SEM. Statistical analysis was performed using one-way ANOVA with Tukey's multiple comparison as post-test

Although there were no statistical differences between samples incubated in different conditions, the TTR samples incubated with plasmin presented higher fluorescence than the TTR samples that were not submitted to proteolysis, indicating more aggregation in the samples digested with plasmin. This slight increase is in line with results from other publications, in which TTR wt presented lower aggregation than TTR V30M or TTR V122I variants treated with plasmin[2,29,47].

TTR samples incubated with plasmin and SerpinA1 presented lower fluorescence than when incubated only with plasmin. Thus, SerpinA1 reduced TTR aggregation possibly due to the inhibition of plasmin proteolytic activity. We did not observe any differences between TTR samples that were not submitted to proteolysis, namely samples incubated in the presence or absence of SerpinA1. Therefore it seems that SerpinA1 does not influence TTR wt aggregation, does not act as chaperone for the TTR wt, contrary to what was described for TTR V122I and TTR V30M[2,47]

We should increase the number of experiments to obtain statistically significant results and should also include other TTR variants like TTRV122I in the assay.

We also performed DLS analysis of the TTR aggregation samples to determine the size distribution of particles in the different protein solutions (Figure 14). Dynamic light scattering (DLS) detect particles as spheres and based on the relative intensity of light scattered, it differentiates particles by diameter[48]. Larger particles scatter more light causing higher intensity of light scattered than small particles[48].

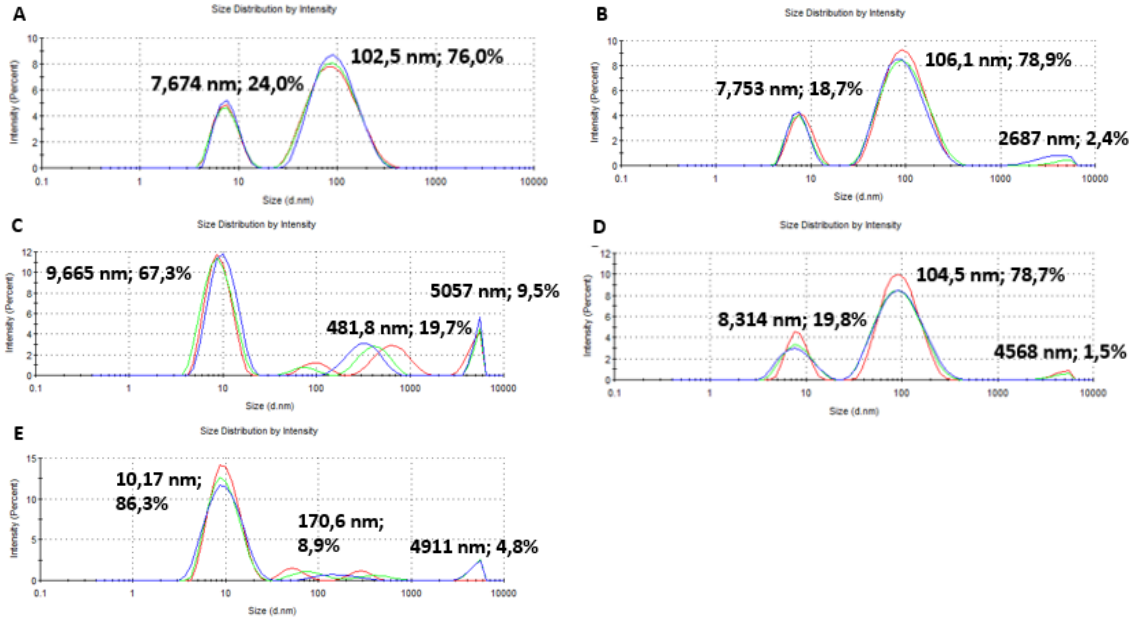

Figure 14 – Effect of proteolysis on TTR wt aggregation analysed by DLS to determine particles size distribution by intensity. **A:** TTR wt at t = 0 hours. **B:** TTR wt at t = 24 hours. **C:** TTR wt with Plasmin at t = 24 hours. **D:** TTR wt sample with SerpinA1 at t = 24 hours. **E:** TTR wt with Plasmin and SerpinA1 t = 24 hours. The values of diameter and intensity percentage represented are means of three measurements for each protein preparation (red, green and blue).

We obtained different classes of particles sizes represented in the graphics “Size Distribution by Intensity” (Figure 14), but all samples presented the native tetrameric soluble form of TTR, a band with 7 to 10 nm of mean diameter. The reference value for TTR is 6 to 7 nm of diameter[49].

The TTR wt sample incubated for 24 hours (Figure 14 **B**) shows a decrease in intensity of the peak representing the size of soluble TTR when compared with sample before incubation t = 0 hours (Figure 14 **A**) which may indicate aggregation. In addition, there is a small increase of the peak at 100 nm and a new small intensity peak appears at more than 1000 nm. These last two peaks should correspond to particles of higher molecular size, possibly oligomers and aggregates.

When TTR wt was incubated in the presence of plasmin (Figure 14 **C**), we observed bands corresponded to larger particles (approximately 500 nm and 5000 nm), consistent with an increase of TTR aggregation when compared with the TTR wt sample incubated for 24 hours alone (Figure 14 **B**).

Regarding aggregation in the presence SerpinA1 (Figure 14 **D**), no significant differences were observed when compared with TTR alone (Figure 14 **B**), in accordance with the results obtained for ThT fluorescence assay. Thus, again SerpinA1 has no chaperone effect on TTR wt aggregation.

When TTR wt was incubated in the presence of both plasmin and SerpinA1 (Figure 14 **E**) larger particles were detected, when compared with TTR wt incubated alone for 24 hours (Figure 14 **B**), but with lower intensity when compared with TTR aggregation in the presence of plasmin (Figure 14 **C**). These results are in line with the ones obtained with ThT fluorescence.

Concerning the peaks corresponding to 100 and 500 nm mean diameter it may correspond to aggregates of TTR wt or complexes formed by the different proteins in the sample: TTR, plasmin and SerpinA1. Also SerpinA1 may be in its dimeric form (15 nm)[50]. Nevertheless, since all samples were submitted to the same conditions, its seems adequate to compare them.

The above mentioned results suggest a reduced proteolytic activity of plasmin over TTR wt. Another evidence of this reduced activity is the fact that TTR fragments were hardly detected by western blot analysis (Figure 15).

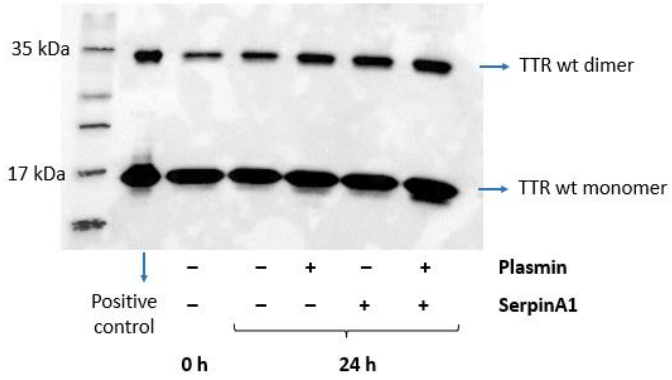

Figure 15 – Investigation of TTR wt fragments in the samples submitted to proteolysis in different conditions. Protein samples were analysed by SDS-PAGE and western blot. The protein samples were the same as those analysed by DLS. No TTR wt fragments were detected with the anti-transthyretin mutant (Y78F), clone AD7 antibody.

A faint band indicating TTR wt fragmentation was detected by the western blot analysis corresponding to TTR aggregation in the presence of plasmin which reinforced both results, of ThT fluorescence and DLS.

4. Effects of aggregated TTR samples under proteolysis in cardiomyocytes

The selection of cardiac cells to study the effect of proteolysis in TTR amyloidosis is related to the fact that fragmented TTR is particularly abundant in amyloid deposits in the heart either in the case of cardiac ATTRv amyloidosis or ATTR wt amyloidosis[51].

Therefore, we performed the assays using the immortalized HL-1 cardiomyocytes cell line to study the effects of the TTR wt in different states of aggregation. Following the characterization of the samples referred to in the previous sections, their effects on HL-1 cardiomyocytes were investigated.

Resazurin was used to determine cell viability (Figure 16), because resazurin is reduced to resorufin by mitochondrial dehydrogenases in live cells, and the amount of resorufin produced is directly proportional to the number of living cells.

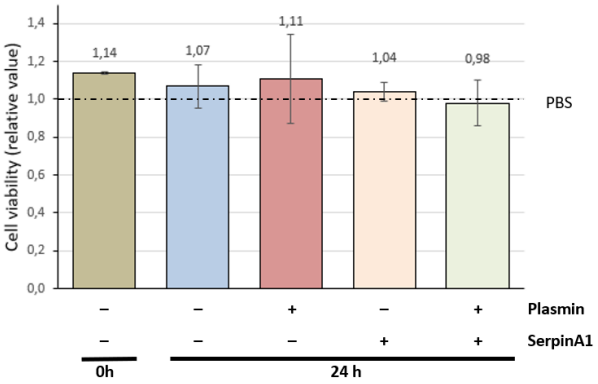

Figure 16 – Viability of HL-1 cardiomyocytes incubated with TTR wt samples in different conditions of aggregation. Live cells reduced Resazurin to resorufin that was evaluated by measurement of fluorescence. Data from one *in vitro* experiment, expressed as mean ± SEM from duplicate analysis, and normalized to the vehicle (PBS), representing the negative control. Statistical analysis was performed using one-way ANOVA with Tukey's multiple comparison as post-test.

We did not observe statistically significant differences in the viability of HL-1 cardiomyocytes incubated with the different TTR wt preparations. These assays should be repeated to confirm the results obtained.

In spite of lack of differences in the cell viability we decided to investigate other biomarkers associated with ATTR amyloidosis.

That is the case of Fas receptor, related to cell death and binding immunoglobulin protein (BiP), the main stress sensor of the endoplasmic reticulum (ER), both found to be increased in cellular and mouse models of the disease as well as in human biopsies from ATTR patients[2]. Another marker analysed was bone morphogenic protein 10 (BMP-10).

BMP-10 is related to cardiomyocytes survival due to its cardioprotective function, and is crucial for normal cardiac development[2,43].

BMP-10 was found downregulated in heart of HM30 mice deficient in HSF (HSF+/- hTTR V30M) especially in older animals and not detectable in plasma of those older mice[43]. In addition, decreased BMP-10 protein levels were reported in cellular studies performed with TTR V122I aggregates[2].

We also evaluated cardiac troponin T (cTnT) as marker of cardiomyocytes functionality.

The results obtained for Fas, BiP, BMP-10 and cTnT by western blot analysis are presented in Figure 17.

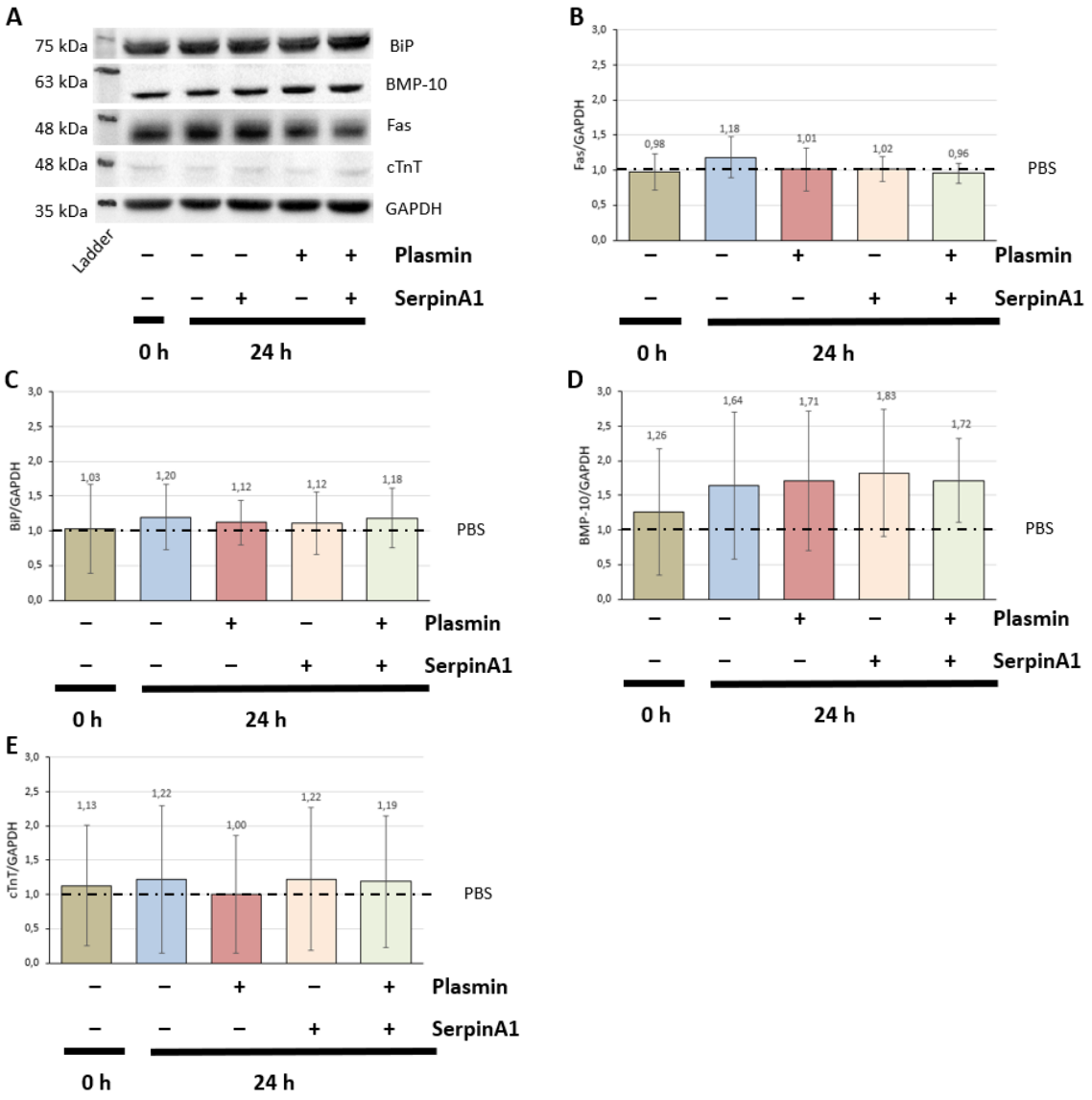

Figure 17 – Evaluation of biomarkers in HL-1 cardiomyocytes incubated (24 hours) with different samples of aggregated TTR. **A:** Cell lysates were analysed by SDS-PAGE and WB using specific antibodies, molecular weights are referred to the ladder. **B-E:** Graphs representing quantification of bands by relative normalized density**. B:** Fas protein levels; **C:** BiP protein levels; **D:** BMP-10 protein levels; **E:** cTnT protein levels. Data from two (n=2) independent *in vitro* experiments,

expressed as mean ± SEM, and normalized to the vehicle (PBS), representing the negative control. GAPDH was used as loading control. Statistical analysis was performed using one-way ANOVA with Tukey's multiple comparison as post-test.

The results obtained show that TTR samples aggregated in different conditions did not alter statistically the levels of the analysed markers as compared to control (vehicle (PBS), 0 hours). This indicated that the TTR samples added to the cells did not induce toxic effects or that at t = 24 hours the cells had recovered homeostasis. The lack of samples toxicity could also indicate low aggregation of TTR due to short time of aggregation (24 hours). We also questioned whether human plasmin and SerpinA1 (present in the samples) might also have influenced the results.

Therefore, we decided to perform similar studies with samples aggregated for longer periods (48 and 120 hours) and to further evaluate aggregation of TTR samples by transmission electron microscopy (TEM). Furthermore, we decided to proceed with TTR samples aggregated without being submitted to proteolysis (without plasmin) however in the next assays we also included a sample of TTR fragment 49-127 to mimic the product of proteolysis and evaluate its aggregation and toxicity to the cells.

5. TTR aggregation analysis without proteolysis

We performed new aggregation assays by incubating the proteins solubilized in PBS at 37ºC and neutral pH, as in the previous assay. We used recombinant TTR wt, TTR L55P, TTR V122I and TTR fragment 49-127, all commercially available. The choice of these proteins was based on their specific characteristics, namely: TTR L55P is a highly amyloidogenic protein that is known to aggregate very rapidly, TTR V122I is a variant associated with a cardiac phenotype, TTR fragment 49-127 is the most common peptide found in amyloid fibrils resulting from proteolysis and TTR wt is our reference protein.

Two experiences were executed with different aggregation times. In one aggregation assay, TTR wt, TTR L55P, TTR V122I and TTR fragment 49-127 were incubated for 48 hours, in the other, TTR wt and TTR L55P were incubated for 120 hours.

Considering the experience of 48 hours of aggregation, we monitored TTR wt, TTR L55P and TTR V122I by ThT fluorescence and TEM at 0, 24 and 48 hours (Figures 18 and 19). TTR fragment 49-127 was only monitored by TEM at 0 hours due to lack of enough material.

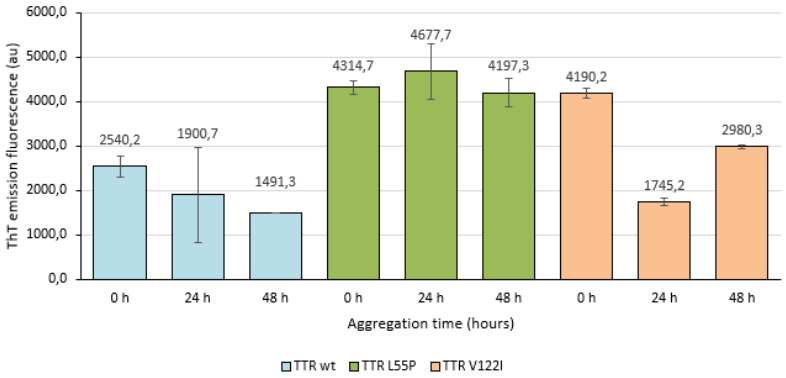

Figure 18 – TTR wt, TTR L55P and TTR V122I aggregation state over 48 hours. Data from one *in vitro* experiment, expressed as mean ± SEM from duplicate analysis.

We observed a decrease in ThT fluorescence for TTR wt. We found it a suspicious result, as we would expect a slight increase of ThT fluorescence or no difference along the 48h of aggregation[17]. For TTR L55P, ThT fluorescence was higher than for the other samples but did not vary much along the 48 hours of the assay. Concerning TTR V122I, there was a decrease of ThT fluorescence at t = 24 and a t = 48 hours though at 24 hours the value was even lower than at 48 hours of aggregation.

Overall, due to lack of consistency of results and considering just tendencies, TTR L55P, the most amyloidogenic form of TTR studied, presented higher levels of ThT fluorescence, followed by TTR V122I (intermediate state of amyloidogenesis) and at last TTR wt (the least amyloidogenic form of the protein studied). However, we cannot conclude about the progression of aggregates formation along time by evaluation of ThT fluorescence.

To obtain more information about the aggregation state of the samples and a morphologic characterization of the species formed during aggregation, samples were analysed by TEM (Figure 19).

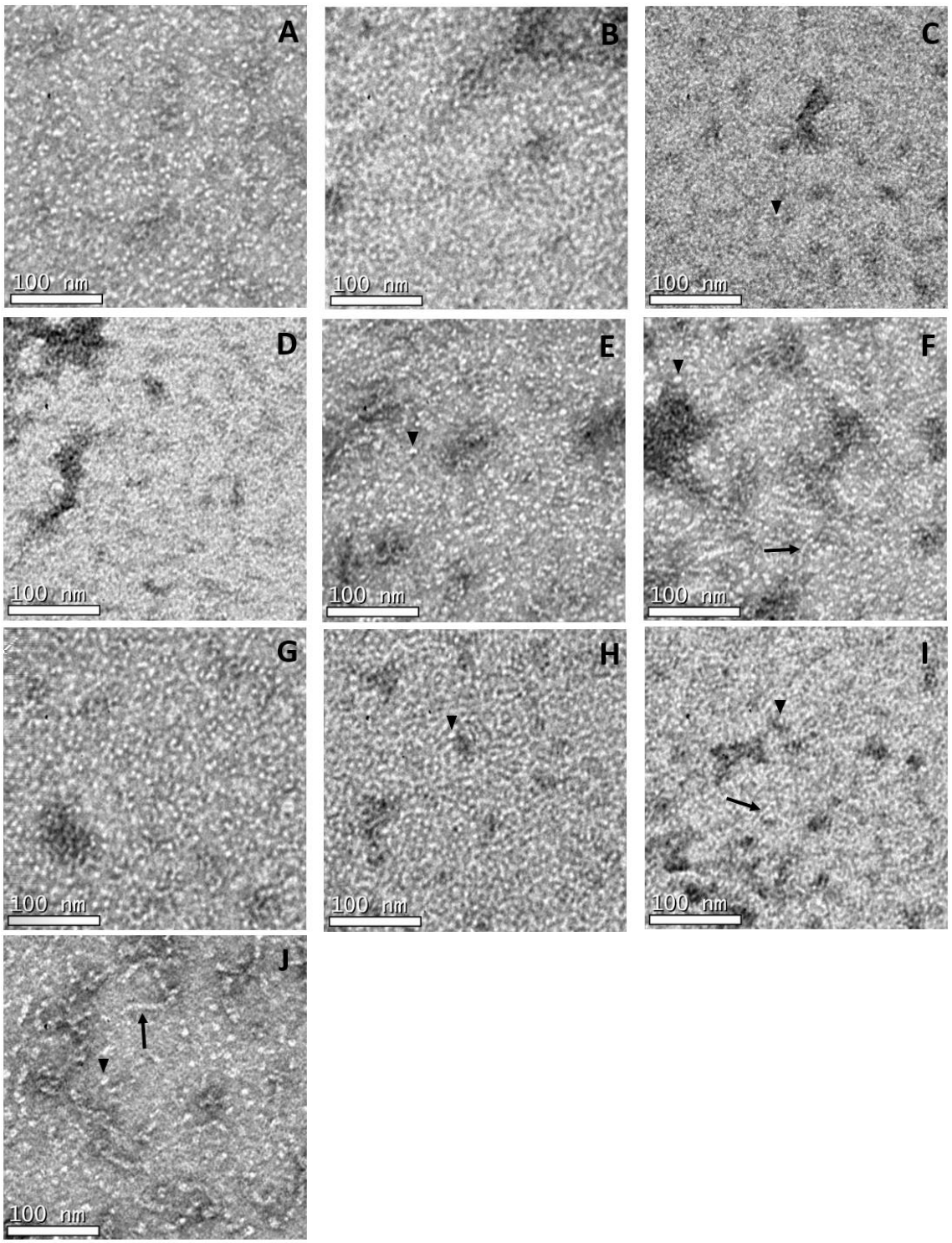

Figure 19 – Transmission electron microscopy of different TTR proteins and TTR fragment used at different time points of aggregation. **A – C:** TTR wt at 0, 24 and 48 hours of aggregation. **D- F:** TTR L55P at 0, 24 and 48 hours of aggregation. **G – I:** TTR V122I at 0, 24 and 48 hours of aggregation; **J:** TTR fragment at 0, 24 and 48 hours of aggregation. Showing the presence of oligomers (arrowhead) or fibrils (arrow).

All protein samples presented small aggregates at 48 hours of aggregation. The results confirmed the amyloidogenic propensity of the different TTR proteins, meaning, TTR L55P presented more aggregates, followed by TTR V122I and finally TTR wt.

Furthermore, TTR L55P presented fibrils at t = 48 hours. Concerning the TTR fragment 49-127, it was only analysed at 0 hours due to lack of sample, but at this time it already presented aggregates and small fibrils confirming its high propensity to aggregate.

These results are more elucidative and show clearly the presence of aggregation in the samples, a result that was not evident in the case of ThT fluorescence determination.

Regarding TTR wt and TTR L55P aggregation for 120 hours, we monitored aggregation by DLS analysis and TEM, once again the limiting factor was the amount of protein available. The results obtained for TTR wt aggregation by DLS at 0, 24 and 120 hours are presented in Figure 20 and TTR L55P was monitored at 0, 24, 72, 96 and 120 hours (Figure 21).

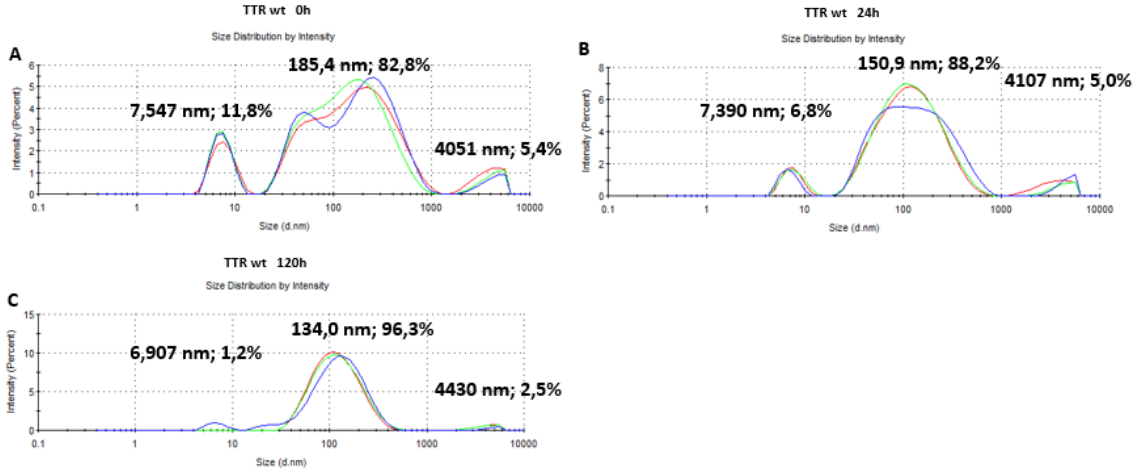

Figure 20 – Effect of proteolysis on TTR wt aggregation analysed by DLS to determine particles size distribution by intensity. **A:** TTR wt at t = 0 hours. **B:** TTR wt at t = 24 hours. **C:** TTR wt at t = 120 hours. The values of diameter and intensity percentage represented are means of the three measurements for each aggregation time (red, green and blue).

A decrease in intensity of particles with small sizes (approximately 10 nm of diameter) and an increase of intensity of particles with approximately 100 nm of diameter was observed, indicating that the soluble tetrameric form of TTR wt was reduced over time and aggregates were formed.

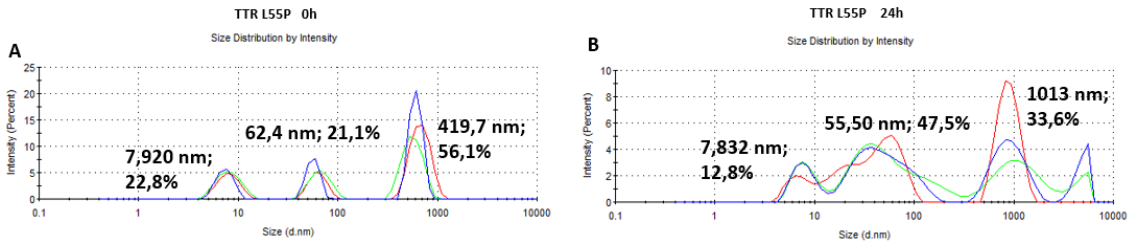

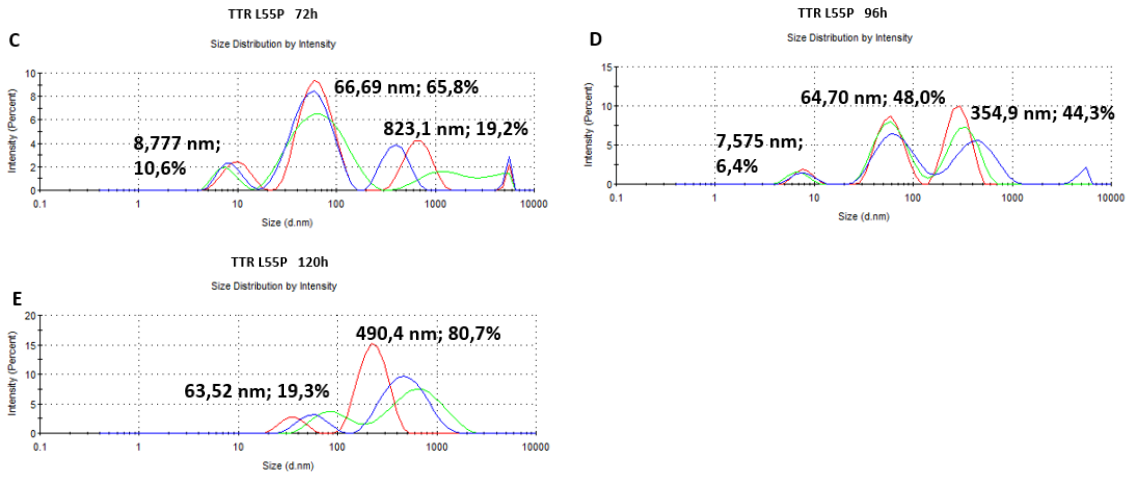

Figure 21 – Effect of proteolysis on TTR L55P aggregation analysed by DLS to determine particles size distribution by intensity. **A:** TTR L55P at t = 0 hours. **B:** TTR L55P at t = 24 hours. **C:** TTR L55P at t = 72 hours. **D:** TTR L55P at t = 96 hours. **E:** TTR L55P at t = 120 hours. The values of diameter and intensity percentage represented are means of the three measurements for each aggregation time (red, green and blue).

TTR L55P presented the same tendency as TTR wt, a decrease of intensity of the band corresponding to the TTR L55P soluble tetrameric form and an increase of intensity of the band corresponding to aggregated TTR. However, the DLS profile of TTR L55P samples presented high heterogeneity of particles of sizes comprising 60 to 800 nm of diameter. This can be explained due to differences in the protein aggregation pathway. TTR L55P presents a more complex aggregation pathway and present different intermediate species, possibly with formation of dimers and trimers as previously suggested by other authors[20].

Transmission electron microscopy (TEM) was performed to visualize the aggregation state of samples (Figure 22). TTR wt aggregation was performed only at 120 hours (Figure 22 **A**) while TTR L55P was analysed at 72, 96 and 120 hours (Figure 22 **B** – **D**).

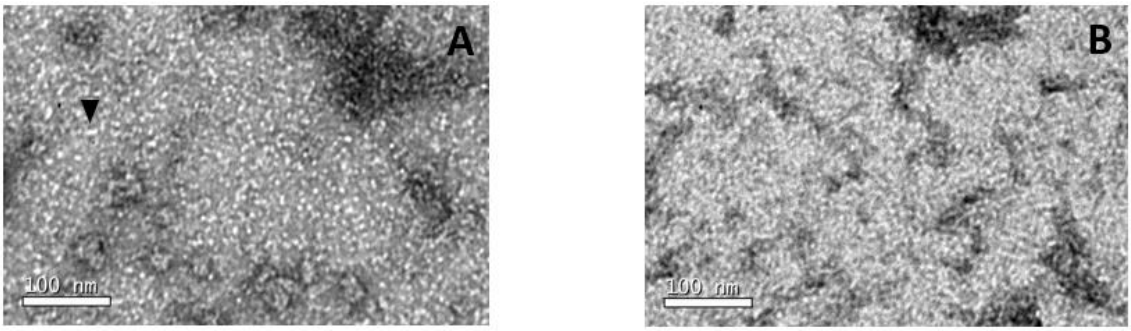

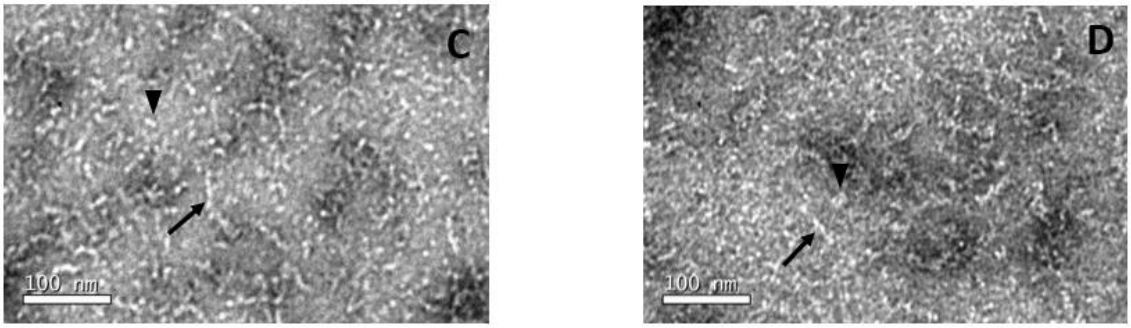

Figure 22 –Transmission electron microscopy of different TTR aggregation states. **A:** TTR wt after 120 hours of incubation at 37 °C. **B:** TTR L55P after 72 hours of incubation at 37 °C. **C:** TTR L55P after 96 hours of incubation at 37 °C. **D:** TTR L55P after 120 hours of incubation at 37 °C. Showing the presence of oligomers (arrowhead) or fibrils (arrow).

We observed oligomerization at 120 hours of aggregation for both proteins. Also, TTR L55P presented larger oligomers and fibrils (Figure 22 **C** and **D**) whereas TTR wt still presented soluble protein (Figure 22 **A**).

Overall, DLS and TEM results are complementary being DLS more informative concerning particles size and abundance while TEM allows morphologic characterization of different species in the sample.

6. Effects of aggregated TTR samples in cardiomyocytes

In the previous section we analysed the aggregation state of the different TTR samples and in this section, we present the results of the effects of those aggregated samples in HL-1 cardiomyocytes.

We analysed HL-1 cardiomyocytes viability after incubation of cells for 3 and 24 hours, at 37 °C, with the TTR protein samples obtained at different aggregation times (Figure 23).

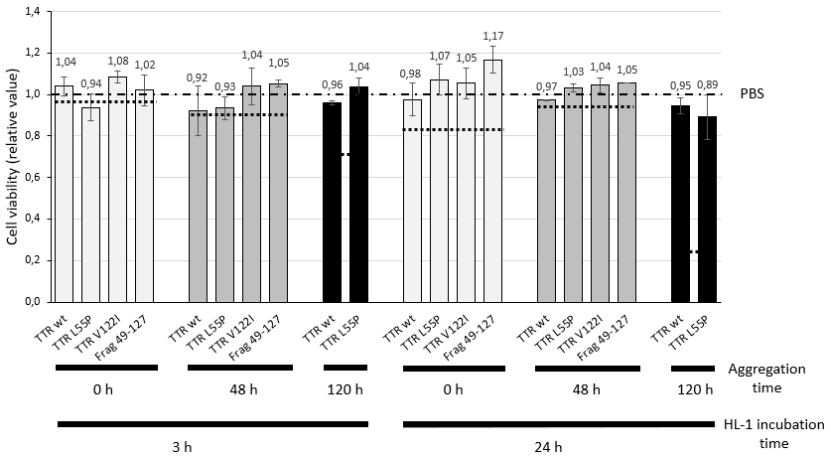

Figure 23 – Effects of different TTR aggregates HL-1 cardiomyocytes' viability. Different protein solutions were incubated for 3 and 24 hours at 37 °C, in 5% CO_2, and were aggregated for 0, 48 and 120 hours. Data from one *in vitro* experiment, expressed as mean ± SEM from duplicate or triplicate analysis, and normalized to the vehicle (PBS), representing the negative control. Statistical analysis was performed using one-way ANOVA with Tukey's multiple comparison as post-test. Dashed lines represent positive control (saponin) relative viability results.

We performed one assay with 2 or 3 replicas of each sample. No statistically significant differences were observed in HL-1 cardiomyocytes viability for the different TTR solutions aggregated for different periods of time (0, 48 and 120 hours) nor at different incubation times (3 and 24 hours). The results indicate that either the different samples do not have any effect on cardiomyocytes or the resazurine assay was not sensitive enough to detect small differences in cellular viability.

In parallel, we analysed the effect of TTR aggregated proteins on cardiomyocytes apoptosis through evaluation of caspases activity (Figure 24). Caspase 3 and caspase 7 activity was detected by luminescence that resulted from caspase cleavage of a substrate which generates a signal produced by luciferase, luminescence is proportional to the amount of caspase activity.

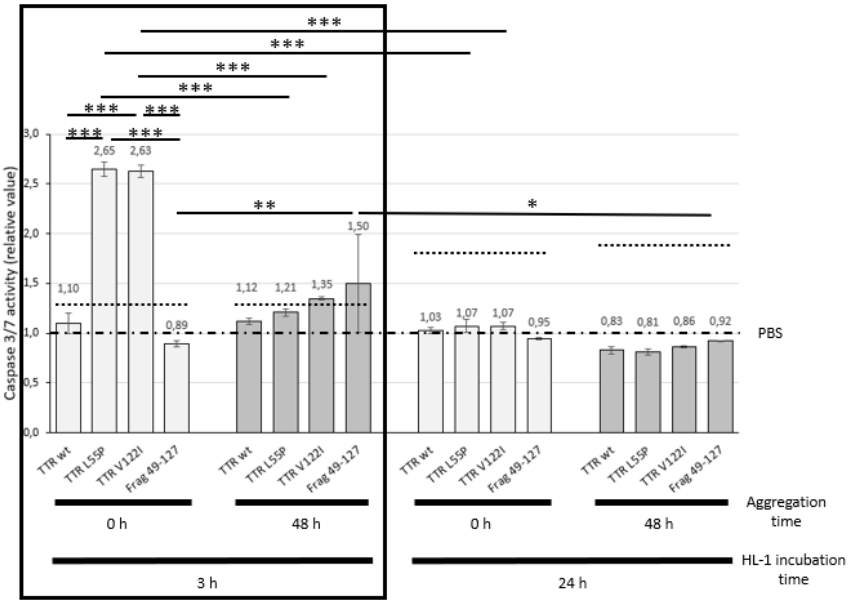

Figure 24 – Effects of different TTR protein solutions on HL-1 cardiomyocytes' caspase 3/7 activity. TTR wt, TTR L55P, TTR V122I and TTR fragment 49-127 were aggregated for 0 and 48 hours and caspase 3/7 activity was measured at 3 and 24 hours of incubation. Data from one *in vitro* experiment, expressed as mean ± SEM from duplicate or triplicate analysis, and normalized to the vehicle (PBS), representing the negative control. Statistical analysis was performed using one-way ANOVA with Tukey's multiple comparison as post-test or t-test. * p<0,05, ** p<0,01, *** p<0,001. Dashed lines represent positive control (staurosporine) relative caspase 3/7 activity results.

Caspase 3/7 activity was higher at shorter incubation period (3 hours) when compared with longer period of cells incubation (24 hours). This indicates that caspases activation is a rapid answer to the aggregated proteins and at longer incubation periods the cells are no longer responding to that stimulus. In addition, caspase activation was particular

high for TTR L55P and TTR V122I at 0 hours of aggregation than at 48 hours suggesting that TTR aggregated samples presenting small oligomers have a higher cytotoxic effects then bigger aggregates and fibrils, which is in line with a previous report for TTR V122I[2]. In accordance, it should be noted that the sample corresponding to TTR fragment 49-127, that as referred in above sections, presented fibrils at time t = 0 hours as analysed by DLS and TEM, did not induce caspases activation in HL-1 cells after 3 hours incubation.

Since we only performed the experiment once, the results should be repeated, to obtain statistically significative results.

We also studied the protein levels of cTnT as it is considered a specific and sensitive marker for myocardial injury[42].

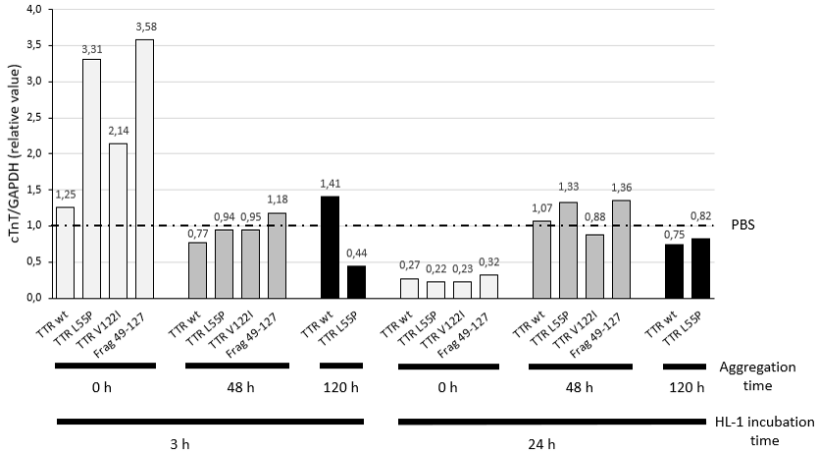

Figure 25 – Biomarker cTnT levels in HL-1 cardiomyocytes. Cells were incubated with the different TTR protein preparations for 3 and 24 hours, at 37 °C, in 5% CO_2. Relative normalized cTnT protein levels. Data from one *in vitro* experiment. Protein levels were normalized to the vehicle (PBS), representing the negative control. GAPDH was used as loading control.

The results obtained (Figure 25) suggest that cells suffered higher damage (lower cTnT) at longer periods of incubation (24 hours) when compared with shorter incubation periods (3 hours). In addition, the effect seems even more evident when comparing TTR aggregated samples at t = 0 hours with different cells incubation periods (3 and 24 hours) indicating that less aggregated samples have higher impact in the HL-1 cells.

Autophagy was demonstrated to be the main regulatory factor in the cardiac homeostasis under basal conditions, since it promotes cardiac adaptation to stress and promotes the clearance of misfolded proteins (in neurodegenerative diseases)[2]. LC3 – I is a cytosolic protein which is cleaved and conjugated with a lipid (phosphatidylethanolamine, PE) and turns into LC3 – II, a membrane bound protein that initiates the autophagosome as well

as its lengthening[2]. LC3 – II/LC3 – I ratio indicates if autophagosome is being formed and/or increasing volume. So, another marker studied was LC3 (Figure 26).

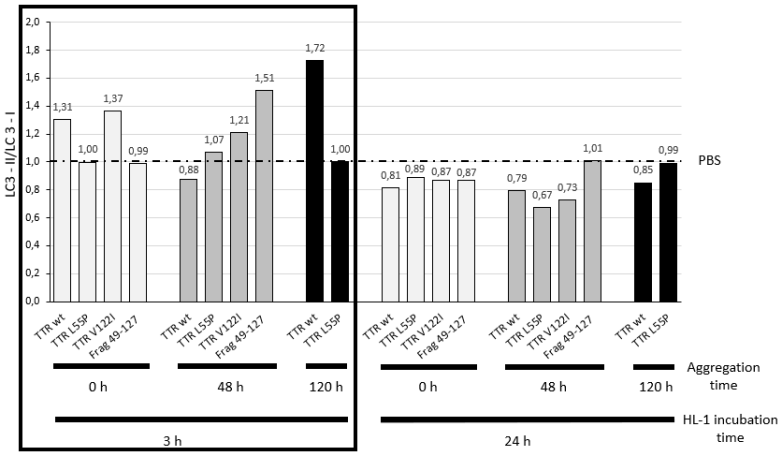

Figure 26 – Biomarker LC3 levels in HL-1 cardiomyocytes. Cells were incubated with the different TTR protein preparations for 3 and 24 hours, at 37 °C, in 5% CO_2. LC3–II/LC3–I protein levels. Data from one *in vitro* experiment.

The ratio LC3 – II/LC3 – I presented higher values when HL-1 cells were incubated with the different aggregated protein solutions for 3 hours than 24 hours, also a more immediate response. Although results were not always consistent with the aggregated state of samples. Nevertheless, generally, autophagy seems to have a more important role in TTR aggregates clearance at shorter periods (3 hours) than longer (24 hours).

We also studied the protein levels of p62 (Figure 27), another autophagy marker. The protein p62 presents its cargo (i.e. misfolded proteins) to LC3 – II, and both, protein and cargo are sequestered in the autophagosome[2,43]. The protein p62 serves as a crucial mediator of aggresome formation and autophagy activation by misfolding proteins in cardiomyocytes[52]

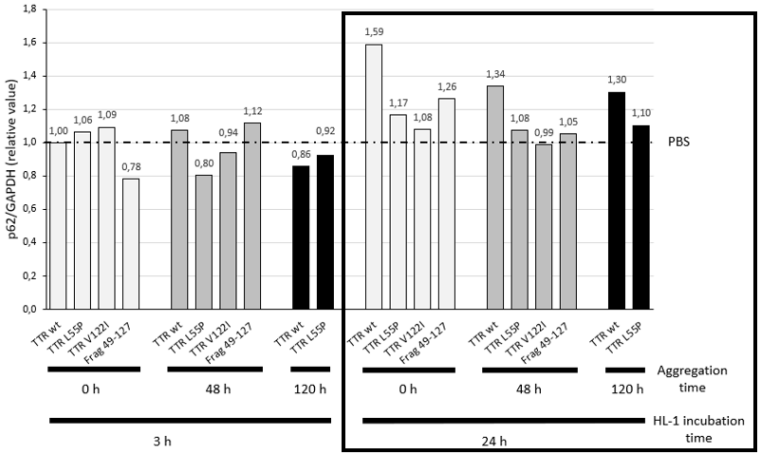

Figure 27 – Biomarker p62 levels in HL-1 cardiomyocytes. Cells were incubated with the different TTR protein preparations for 3 and 24 hours, at 37 °C, in 5% CO_2. Relative normalized p62 protein levels. Data from one *in vitro* experiment. Protein levels were normalized to the vehicle (PBS), representing the negative control. GAPDH was used as loading control.

The presenting cargo protein p62 levels were higher when HL-1 cells were incubated with the different aggregated protein solutions for 24 hours, showing a later response to the aggregated samples indicating increased autophagy.

We also analysed the ER stress sensor BiP (Figure 28).

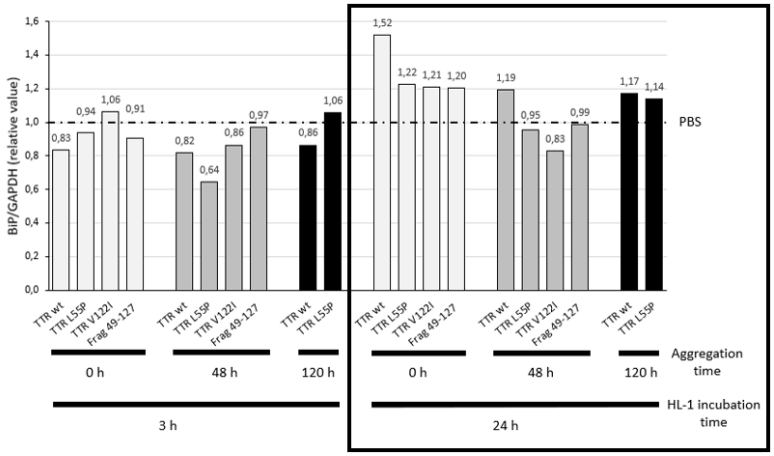

Figure 28 – Biomarker BiP levels in HL-1 cardiomyocytes. Cells were incubated with the different TTR protein preparations for 24 hours, at 37 °C, in 5% CO_2. Relative normalized BiP protein levels. Data from one *in vitro* experiment. Protein levels were normalized to the vehicle (PBS), representing the negative control. GAPDH was used as loading control.

The ER stress sensor, BiP, presented higher relative levels, when HL-1 cells were incubated with the different aggregated protein solutions for 24 hours than 3 hours and again the less aggregated TTR samples have a higher impact in BiP levels when compared for the same cellular incubation period.

Overall, cellular studies presented a high variability and were not completely consistent, we shall repeat them. We shall also perform qRT-PCR to analyse the expression of these markers to complement the data from the protein levels. Inconsistencies in protein quantifications may be related with the fact that western blot analysis is not a very precise technique.

Conclusions

The main objective of this project was to contribute to the elucidation of the mechanisms involved in TTR amyloidosis and its modulation. Previous studies from our group and also from other research groups indicated that SerpinA3/Serpina3n could play a role in TTR amyloidosis. Thus, based on alterations of SerpinA3 levels in TTR V30M patients but also on alterations in the Serpina3n in the HM30 mice model of the disease we investigated Serpina3n mRNA and protein levels in the liver and heart and also protein levels in the plasma of HM30 mice and compared them with wild type mice (IW). We found similar expression levels of Serpina3n mRNA in both, liver and heart tissues, although, protein levels were found decreased in the liver. Concerning Serpina3n in plasma, HM30 mice presented higher levels than controls (IW), which could be due to increased Serpina3n secretion from liver associated with its role as extracellular chaperone, as a TTR chaperone in ATTR amyloidosis. Interestingly, SerpinA3 plasma levels are decreased in polyneuropathy patients, TTR V30M patients. This might suggest that TTR V30M patients present an impaired chaperone system or the differences found in SerpinA3 levels are associated with other conditions of patients namely age and gender. Since we only studied mice of 12-15 months old, we should study Serpina3n and TTR levels in groups of mice of different ages, namely younger (4-6 months) and older (18-24 months), consider groups by gender and increase number of individuals by group.

Besides its role as extracellular chaperones, serpins are inhibitors of serine proteases and as such, might also play a role in ATTR amyloidosis through modulation of TTR proteolysis one of the mechanisms contributing to TTR aggregation. TTR proteolysis has been considered particularly relevant in ATTR cardiac amyloidosis thus we conducted studies of TTR aggregation in different conditions of proteolysis and tested the aggregated solutions in cardiac cells, in particular HL-1 cardiomyocytes. We performed studies of TTR aggregation in the presence of plasmin.

Regarding the aggregation studies, when TTR wt aggregation was performed in proteolytic conditions, we confirmed the reduced plasmin activity with TTR wt. We also found that the effect of SerpinA1 is probably due to inhibition of plasmin instead of acting as a TTR wt chaperone. Considering the influence of the different aggregated species in HL-1 cardiomyocytes, no differences were observed in the levels of the different disease markers studied, suggesting that 24 hours of aggregation were not sufficient to form enough small TTR wt aggregates (confirmed by the DLS analysis) that could perturb the cell homeostasis.

Plasmin was used as proteolytic enzyme because it was previously identified as a possible protease involved in TTR amyloidosis, since it triggers amyloid formation *in vitro* and promotes amyloid deposition in a mouse transgenic model[29,30]. Nevertheless, other proteases may be involved in the process of TTR proteolysis as subtilisin[53]. Subtilisin is a serine protease from Bacillus subtilis, a nonpathogenic microbe in the gut, and with the increased gut permeability during aging, subtilisin levels into the human plasma may increase, and may contribute to the pathogenesis of ATTRwt amyloidosis[53]. Or else, other proteases, presently not identified, can be involved in TTR wt proteolysis instead, or additionally, to plasmin.

It was suggested that SerpinA1 may act as chaperone influencing TTR amyloid formation because SerpinA1 levels were found to be overrepresented in serum from TTR V30M patients. Furthermore, studies of HM30 mice revealed that Serpina1a knockdown through anti-sense oligomers resulted in increased plasmin proteolytic activity in plasma and increased deposition of aggregated TTR V30M in several tissues including the heart[28,47,54]. TTR fragments were observed in the heart[28,47,54]. Nevertheless, SerpinA1 does not seem to interact directly with TTR wt.

Analyses of TTR proteins aggregation without proteolysis confirmed the amyloidogenic propensity of the different TTR variants including the TTR 49-127 fragment. This peptide allowed to study the aggregation properties and effects of the TTR fragment without the presence of the protease (plasmin). The aggregation studies mainly by DLS and TEM demonstrated that the fragment was the most amyloidogenic protein followed by TTR L55P, TTR V122I and TTR wt. All the protein samples presented high complexity in what concerns the different oligomeric species in solution. Though, TTR 49-127 fragment was mainly composed by fibrils even at t = 0 hours as was evident by TEM confirming its high potential to aggregate and its relevance in amyloid formation. The heterogeneity of composition of protein samples certainly contributes to the variability of results obtained while evaluating markers of toxicity. Nevertheless, samples with less aggregation and smaller oligomeric species induced higher cytotoxicity as evident by rapid (3 hours) increased of caspase 3/7 activation and thus higher apoptosis followed by increased damage of cardiomyocytes correlated with cTnT decrease in a later stage (24 hours).

We found that autophagy is implicated in the initial response (3 hours) to the aggregated proteins in the case of ratio LC3 – II/LC3 – I, a higher effect was observed for the highly aggregated fragment TTR 49-127. A latter response (24 hours) of cells involves the increase of the presenting cargo protein (increased p62). At this advanced stage of

autophagy higher levels of BiP indicated increased ER stress. In an early phase the effect on ER stress was not observed because it might be attenuated by activation of autophagy[55].

These *in vitro* and cellular studies have limitations. We used isolated proteins which were subject to the same aggregation conditions, what does not happen *in vivo*, additionally, aggregates and fibrils are not only composed by TTR neither by the same TTR species. Also, we could not control the aggregation state of the oligomers, and in the case of the TTR fragment 49-127, it was already aggregated (at t = 0 hours). *In vivo*, not all protein is cleaved and the kinetics of fragment aggregation may vary according to tissue specificity. Furthermore, *in vivo* intermediate species that we do not observe or identify *in vitro* can be present. Another limitation is to precisely mimic factors as concentration, the kinetics of the process (TTR dissociation and amyloid formation) or physiologic environment where aggregation occurs.

Despite all limitations of *in vitro* and cellular studies, they are important for the detailed knowledge of the TTR mechanism of aggregation, since the involvement of specific factors can be targeted for modulation aiming therapeutic approaches and simple systems permit to identify such factors and allow to test modulators.

References

1. Bezerra, F., Saraiva, M. J. & Almeida, M. R. Modulation of the Mechanisms Driving Transthyretin Amyloidosis. *Front. Mol. Neurosci.* **13**, 592644 (2020).

2. Bezerra, F. Modulation of mechanisms driving TTR amyloidogenesis: from tetramer destabilization to TTR proteolysis. (Porto, 2022).

3. Wentink, A., Nussbaum-Krammer, C. & Bukau, B. Modulation of Amyloid States by Molecular Chaperones. *Cold Spring Harb. Perspect. Biol.* **11**, (2019).

4. Westermark, G. T., Fändrich, M., Lundmark, K. & Westermark, P. Noncerebral Amyloidoses: Aspects on Seeding, Cross-Seeding, and Transmission. *Cold Spring Harb. Perspect. Med.* **8**, (2018).

5. Luigetti, M., Romano, A., Di Paolantonio, A., Bisogni, G. & Sabatelli, M. Diagnosis and Treatment of Hereditary Transthyretin Amyloidosis (hATTR) Polyneuropathy: Current Perspectives on Improving Patient Care. *Ther. Clin. Risk Manag.* **16**, 109–123 (2020).

6. Ueda, M. Transthyretin: Its function and amyloid formation. *Neurochem. Int.* **155**, 105313 (2022).

7. Obi, C. A., Mostertz, W. C., Griffin, J. M. & Judge, D. P. ATTR Epidemiology, Genetics, and Prognostic Factors. *Methodist Debakey Cardiovasc. J.* **18**, 17–26 (2022).

8. Inomata, T. *et al.* Diagnosis of wild-type transthyretin amyloid cardiomyopathy in Japan: red-flag symptom clusters and diagnostic algorithm. *ESC Hear. Fail.* **8**, 2647–2659 (2021).

9. Tanskanen, M. *et al.* Senile systemic amyloidosis affects 25% of the very aged and associates with genetic variation in alpha2-macroglobulin and tau: a population-based autopsy study. *Ann. Med.* **40**, 232–239 (2008).

10. Ueda, M. *et al.* Clinicopathological features of senile systemic amyloidosis: an ante- and post-mortem study. *Mod. Pathol. an Off. J. United States Can. Acad. Pathol. Inc* **24**, 1533–1544 (2011).

11. Maurer, M. S. *et al.* Expert Consensus Recommendations for the Suspicion and Diagnosis of Transthyretin Cardiac Amyloidosis. *Circ. Heart Fail.* **12**, e006075 (2019).

12. Adams, D. *et al.* Expert consensus recommendations to improve diagnosis of ATTR amyloidosis with polyneuropathy. *J. Neurol.* **268**, 2109–2122 (2021).

13. Mutations in Hereditary Amyloidosis. http://www.amyloidosismutations.com/mut-attr.php (2015).

14. Finsterer, J. *et al.* Hereditary transthyretin-related amyloidosis. *Acta Neurol. Scand.* **139**, 92–105 (2019).

15. Ibrahim, R. B., Liu, Y.-T., Yeh, S.-Y. & Tsai, J.-W. Contributions of Animal Models to the Mechanisms and Therapies of Transthyretin Amyloidosis. *Front. Physiol.* **10**, 338 (2019).

16. Dasari, A. K. R. *et al.* Disruption of the CD Loop by Enzymatic Cleavage Promotes the Formation of Toxic Transthyretin Oligomers through a Common Transthyretin Misfolding Pathway. *Biochemistry* **59**, 2319–2327 (2020).

17. Ueda, M. *et al.* A cell-based high-throughput screening method to directly examine transthyretin amyloid fibril formation at neutral pH. *J. Biol. Chem.* **294**, 11259–11275 (2019).

18. Hendren, N. S., Roth, L. R. & Grodin, J. L. Disease-Specific Biomarkers in Transthyretin Cardiac Amyloidosis. *Curr. Heart Fail. Rep.* **17**, 77–83 (2020).

19. Magalhães, J., Eira, J. & Liz, M. A. The role of transthyretin in cell biology: impact on human pathophysiology. *Cell. Mol. Life Sci.* **78**, 6105–6117 (2021).

20. Hurshman Babbes, A. R., Powers, E. T. & Kelly, J. W. Quantification of the thermodynamically linked quaternary and tertiary structural stabilities of transthyretin and its disease-associated variants: the relationship between stability and amyloidosis. *Biochemistry* **47**, 6969–6984 (2008).

21. Hörnberg, A., Eneqvist, T., Olofsson, A., Lundgren, E. & Sauer-Eriksson, A. E. A comparative analysis of 23 structures of the amyloidogenic protein transthyretin. *J. Mol. Biol.* **302**, 649–669 (2000).

22. Si, J.-B., Kim, B. & Kim, J. H. Transthyretin Misfolding, A Fatal Structural Pathogenesis Mechanism. *Int. J. Mol. Sci.* **22**, (2021).

23. Sant'Anna, R. *et al.* The importance of a gatekeeper residue on the aggregation of transthyretin: implications for transthyretin-related amyloidoses. *J. Biol. Chem.* **289**, 28324–28337 (2014).

24. Hammarström, P., Jiang, X., Hurshman, A. R., Powers, E. T. & Kelly, J. W. Sequence-dependent denaturation energetics: A major determinant in amyloid disease diversity. *Proc. Natl. Acad. Sci. U. S. A.* **99 Suppl 4**, 16427–16432 (2002).

25. Suhr, O. B., Lundgren, E. & Westermark, P. One mutation, two distinct disease variants: unravelling the impact of transthyretin amyloid fibril composition. *J. Intern. Med.* **281**, 337–347 (2017).

26. Suhr, O. B. *et al.* Amyloid fibril composition within hereditary Val30Met (p. Val50Met) transthyretin amyloidosis families. *PLoS One* **14**, e0211983 (2019).

27. Marcoux, J. *et al.* A novel mechano-enzymatic cleavage mechanism underlies transthyretin amyloidogenesis. *EMBO Mol. Med.* **7**, 1337–1349 (2015).

28. da Costa, G. *et al.* Transthyretin Amyloidosis: Chaperone Concentration Changes and Increased Proteolysis in the Pathway to Disease. *PLoS One* **10**, e0125392 (2015).

29. Mangione, P. P. *et al.* Plasminogen activation triggers transthyretin amyloidogenesis in vitro. *J. Biol. Chem.* **293**, 14192–14199 (2018).

30. Slamova, I. *et al.* Plasmin activity promotes amyloid deposition in a transgenic model of human transthyretin amyloidosis. *Nat. Commun.* **12**, 7112 (2021).

31. Miszta, A. *et al.* Assessing Plasmin Generation in Health and Disease. *Int. J. Mol. Sci.* **22**, (2021).

32. Keragala, C. B. & Medcalf, R. L. Plasminogen: an enigmatic zymogen. *Blood* **137**, 2881–2889 (2021).

33. Sánchez-Navarro, A., González-Soria, I., Caldiño-Bohn, R. & Bobadilla, N. A. An integrative view of serpins in health and disease: the contribution of SerpinA3. *Am. J. Physiol. Cell Physiol.* **320**, C106–C118 (2021).

34. Aslam, M. S. & Yuan, L. Serpina3n: Potential drug and challenges, mini review. *J. Drug Target.* **28**, 368–378 (2020).

35. Heit, C. *et al.* Update of the human and mouse SERPIN gene superfamily. *Hum. Genomics* **7**, 22 (2013).

36. Chan, G. G., Koch, C. M. & Connors, L. H. Serum Proteomic Variability Associated with Clinical Phenotype in Familial Transthyretin Amyloidosis (ATTRm). *J. Proteome Res.* **16**, 4104–4112 (2017).

37. Padilla-Godínez, F. J. *et al.* Protein Misfolding and Aggregation: The Relatedness between Parkinson's Disease and Hepatic Endoplasmic Reticulum Storage Disorders. *Int. J. Mol. Sci.* **22**, (2021).

38. Foil, K. E. Variants of SERPINA1 and the increasing complexity of testing for alpha-1 antitrypsin deficiency. *Ther. Adv. Chronic Dis.* **12_suppl**, 20406223211015950 (2021).

39. Kohno, K. *et al.* Analysis of amyloid deposition in a transgenic mouse model of homozygous familial amyloidotic polyneuropathy. *Am. J. Pathol.* **150**, 1497–1508 (1997).

40. Furuya, H. *et al.* Production of recombinant human transthyretin with biological activities toward the understanding of the molecular basis of familial amyloidotic polyneuropathy (FAP). *Biochemistry* **30**, 2415–2421 (1991).

41. Tran, M., Wu, J., Wang, L. & Shin, D.-J. A Potential Role for SerpinA3N in Acetaminophen-Induced Hepatotoxicity. *Mol. Pharmacol.* **99**, 277–285 (2021).

42. Kristen, A. V *et al.* Impact of genotype and phenotype on cardiac biomarkers in patients with transthyretin amyloidosis - Report from the Transthyretin Amyloidosis Outcome Survey (THAOS). *PLoS One* **12**, e0173086 (2017).

43. Teixeira, C. The contribution of an animal model for the pathogenetic characterization and therapeutic approaches in ATTR cardiac amyloidosis. (Porto, 2021).

44. Ridge, K. M., Eriksson, J. E., Pekny, M. & Goldman, R. D. Roles of vimentin in health and disease. *Genes Dev.* **36**, 391–407 (2022).

45. Tsikitis, M., Galata, Z., Mavroidis, M., Psarras, S. & Capetanaki, Y. Intermediate filaments in cardiomyopathy. *Biophys. Rev.* **10**, 1007–1031 (2018).

46. MacLean, J. & Pasumarthi, K. B. S. Characterization of primary adult mouse cardiac fibroblast cultures. *Can. J. Physiol. Pharmacol.* **98**, 861–869 (2020).

47. Bezerra, F. *et al.* In Vitro and In Vivo Effects of SerpinA1 on the Modulation of Transthyretin Proteolysis. *Int. J. Mol. Sci.* **22**, (2021).

48. *Dynamic Light Scattering : An Introduction in 30 Minutes*. (2014).

49. Groenning, M., Campos, R. I., Hirschberg, D., Hammarström, P. & Vestergaard, B. Considerably Unfolded Transthyretin Monomers Preceed and Exchange with

Dynamically Structured Amyloid Protofibrils. *Sci. Rep.* **5**, 11443 (2015).

50. Bashir, A. *et al.* Aggregation of M3 (E376D) variant of alpha1- antitrypsin. *Sci. Rep.* **10**, 8290 (2020).

51. Misumi, Y., Ando, Y. & Ueda, M. Early transverse tubule involvement in cardiomyocytes in hereditary transthyretin amyloidosis: a possible cause of cardiac events. *Cardiovasc. Pathol. Off. J. Soc. Cardiovasc. Pathol.* **61**, 107458 (2022).

52. Zheng, Q., Su, H., Ranek, M. J. & Wang, X. Autophagy and p62 in cardiac proteinopathy. *Circ. Res.* **109**, 296–308 (2011).

53. Gonzalez-Duarte, A. & Ulloa-Aguirre, A. A Brief Journey through Protein Misfolding in Transthyretin Amyloidosis (ATTR Amyloidosis). *Int. J. Mol. Sci.* **22**, (2021).

54. Niemietz, C. *et al.* SERPINA1 modulates expression of amyloidogenic transthyretin. *Exp. Cell Res.* **395**, 112217 (2020).

55. Chipurupalli, S., Samavedam, U. & Robinson, N. Crosstalk Between ER Stress, Autophagy and Inflammation. *Front. Med.* **8**, 758311 (2021).